Progress in Polymer Science 34 (2009) 125–155

Contents lists available at ScienceDirect

Progress in Polymer Science

journal homepage: www.elsevier.com/locate/ppolysci

Nano-biocomposites: Biodegradable polyester/nanoclay systems

Perrine Bordes, Eric Pollet, Luc Avérous*

LIPHT-ECPM, UMR 7165, Université de Strasbourg, 25 rue Becquerel, 67087 Strasbourg Cedex 2, France

ARTICLE INFO

Article history:
Received 1 June 2008
Received in revised form 27 October 2008
Accepted 28 October 2008
Available online 14 November 2008

Keywords:
Biopolyesters
Nano-biocomposites
Clay
Biodegradable

ABSTRACT

In the recent years, bio-based products have raised great interest since sustainable development policies tend to expand with the decreasing reserve of fossil fuel and the growing concern for the environment. Consequently, biopolymers, i.e., biodegradable polymers, have been the topic of many researches. They can be mainly classified as agro-polymers (starch, protein, etc.) and biodegradable polyesters (polyhydroxyalkanoates, poly(lactic acid), etc.). These latter, also called biopolyesters, can be synthesized from fossil resources but main productions are obtained from renewable resources. Unfortunately for certain applications, biopolyesters cannot be fully competitive with conventional thermoplastics since some of their properties are too weak. Therefore, to extend their applications, these biopolymers have been formulated and associated with nano-sized fillers, which could bring a large range of improved properties (stiffness, permeability, crystallinity, thermal stability). The resulting 'nano-biocomposites' have been the subject of many recent publications. This review is dedicated to this novel class of materials based on clays, which are nowadays the main nanofillers used in nanocomposites systems. This review highlights the main researches and developments in biopolyester/nanoclay systems during the last decade.

Contents

* Corresponding author. Tel.: +33 3 90 242 707; fax: +33 3 90 242 716.
E-mail address: AverousL@ecpm.u-strasbg.fr (L. Avérous).

0079-6700/$ – see front matter © 2008 Elsevier Ltd. All rights reserved.
doi:10.1016/j.progpolymsci.2008.10.002

1. Introduction

In recent years biopolymers, i.e., biodegradable polymers, have attracted more and more interest due to increasing environmental concern and decreasing fossil resources. This evolution motivates academic and industrial research to develop novel materials labelled as "environmentally-friendly", i.e., materials produced from alternative resources, with lower energy consumption, biodegradable and non-toxic to the environment. Since biopolymers are biodegradable and the main productions are obtained from renewable resources such as agro-resources, they represent an interesting alternative route to common non-degradable polymers for short-life range applications (packaging, agriculture, etc.). Nevertheless, until now, most biopolymers are costly compared to conventional thermoplastic and they are sometimes too weak for practical use. Therefore, it appears necessary to improve these biopolymers to make them fully competitive with common thermoplastics.

Nanocomposites are novel materials with drastically improved properties due to the incorporation of small amounts (less than 10 wt%) of nano-sized fillers into a polymer matrix. Nanofillers can be classified according to their morphology, such as particles that are (i) layered (e.g., clays), (ii) spherical (e.g., silica) or (iii) acicular (e.g., whiskers, carbon nanotubes). Their specific geometrical dimensions, and thus aspect ratios, partly affect the final materials properties. Layered silicate clays offer high surface area, more than 700 m^2/g, i.e., a huge interface with the polymer (matrix), which governs the material properties. The final behavior can be considerably improved by the strong and extensive polymer–nanofiller interactions, as well as, good particle dispersion.

Nano-biocomposites are obtained by adding nanofillers to biopolymers, resulting in very promising materials since they show improved properties with preservation of the material biodegradability, without eco-toxicity. Such materials are mainly destined to biomedical applications and different short-term applications, e.g., packaging, agriculture or hygiene devices. They thus represent a strong and emerging answer for improved and eco-friendly materials. Although few articles were published on this topic during the last century, but numerous publications have already appeared since that time.

This review reports on an aspect of the state of the art in wide field of nano-biocomposites materials, namely to nano-biocomposites based on biopolyester/clay systems. Layered silicates are widely used in nanocomposites systems and biopolyesters are currently the most promising biopolymers for wide range of important applications. The first part describes several biopolymers, focusing on the origins and characteristics of the principal biopolyesters. In the second part, the structure and properties of nano-biocomposites based on biopolyester/clays systems are reported in detail.

2. Biodegradable polymers classification

A vast number of biodegradable polymers (biopolymers) are chemically synthesized or biosynthesized during the growth cycles of all organisms. Some micro-organisms and enzymes capable of degrading them have been identified [1–4]. Fig. 1 proposes a classification with four different categories, depending on the synthesis [5]:

(a) polymers from biomass such as the agro-polymers from agro-resources, e.g., starch, cellulose,
(b) polymers obtained by microbial production, e.g., the polyhydroxyalkanoates,
(c) polymers chemically synthesized using monomers obtained from agro-resources, e.g., poly(lactic acid),
(d) polymers whose monomers and polymers are both obtained by chemical synthesis from fossil resources.

Of these, only categories (a)–(c) are obtained from renewable resources. We can sort these different biodegradable polymers into two main families, the agro-polymers (category a) and the biodegradable polyesters (categories b–d), also called biopolyesters.

3. Biodegradable polyesters

Table 1 and Fig. 2 show the chemical structures, trade names and main properties of commercially available biopolyesters.

3.1. Polyesters based on agro-resources

3.1.1. Poly(lactic acid)

Lactic acid is a chiral molecule existing as two stereoisomers, L- and D-lactic acid which can be produced in different ways, i.e., biologically or chemically synthesized [6].

In the first case, lactic acid is obtained by fermentation of carbohydrates from lactic bacteria, belonging mainly to the genus *Lactobacillus*, or fungi [7,8]. This fermentative pro-

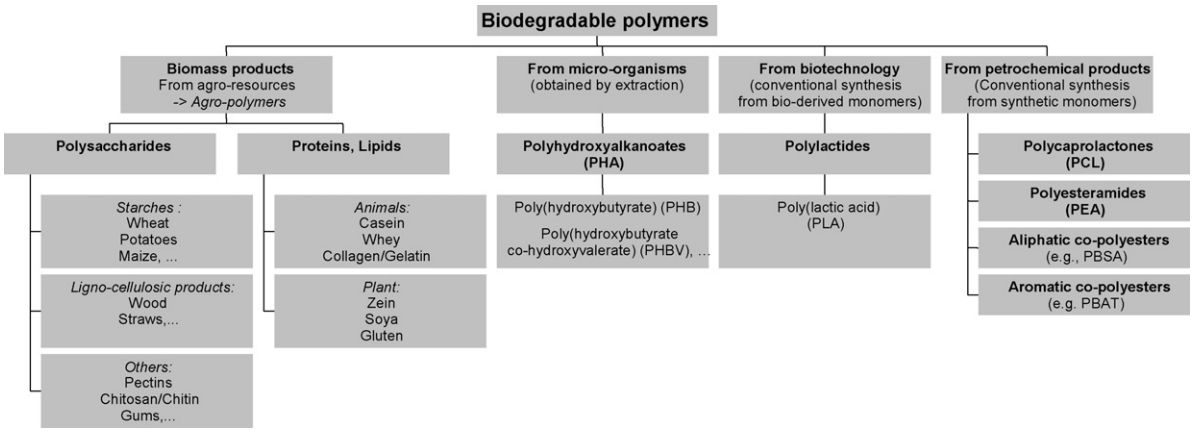

Fig. 1. Classification of the biodegradable polymers. Reproduced with permission from Averous [190] copyright (2004) of Marcel Dekker, Inc.

cess requires a bacterial strain but also sources of carbon (carbohydrates), nitrogen (yeast extract, peptides, etc.) and mineral elements to allow the growth of bacteria and the production of lactic acid. The lactic acid as-formed exists almost exclusively as L-lactic acid and leads to poly(L-lactic acid) PLLA with low molecular weight by polycondensation reaction. However, Moon et al. [9,10] have proposed an alternative solution to obtain higher molecular weight PLLA by the polycondensation route.

In contrast, the chemical process could lead to various ratio of L- and D-lactic acid. Indeed, the chemical reactions leading to the formation of the cyclic dimer, the lactide, as an intermediate step to the production of PLA, could lead to macromolecular chains with L- and D-lactic acid monomers. This mechanism of ring-opening polymerization ROP from the lactide explains the formation of two enantiomers. This ROP route has the advantage of reaching high molecular weight polymers [1,7,11,12] and allows control of the PLA final properties by adjusting the proportions and the sequencing of L- and D-lactic acid units.

At present, due to its availability on the market and its low price [13–16], PLA has one of the highest potentials among biopolyesters, particularly for packaging [14,16] and medical applications. For instance, Cargill has developed processes that use corn and other feedstock to produce different PLA grades (NatureWorks®) [15,17]. For this company, the actual production is estimated to 50–60 ktons per year although the production capacity is given at 140 ktons (http://www.natureworksllc.com). However, presently, it is the highest and worldwide production of biodegradable polyester. Its price was around 2€/kg in 2006, but nowadays the cost has slightly increased. Different companies such as Mitsui Chemicals (Japan), Mitsubishi (Japan), Biomer (Germany), Shimadzu (Japan), Galactic-Total (Belgium), Toyota (Japan), Purac (Netherlands), Treofan (Netherlands) or Dainippon Ink Chemicals (Japan) produce smaller PLAs outputs with different D/L ratios. Commercially available, we can find 100% PLLA which present a high crystallinity C-PLA and copolymers of PLLA and poly(D,L-lactic acid) PDLLA which are rather amorphous A-PLA [17–19]. PLA can show crystalline polymorphism [20] which can lead

Table 1
Physical data of some commercial biopolyesters. Reproduced with permission from Averous [190] copyright (2004) of Marcel Dekker, Inc.

	PLA Dow–Cargill (NatureWorks)	PHBV Monsanto (Biopol D400G – HV = 7 mol%)	PCL Solvay (CAPA 680)	PEA Bayer (BAK 1095)	PBSA Showa (Bionolle 3000)	PBAT Eastman (Eastar bio 14766)
Density	1.25	1.25	1.11	1.07	1.23	1.21
Melting point (°C)[a]	152	153	65	112	114	110–115
Glass transition (°C)[a]	58	5	−61	−29	−45	−30
Crystallinity[b] (in %)	0–1	51	67	33	41	20–35
Modulus (MPa) (NFT 51-035)	2050	900	190	262	249	52
Elongation at break (%) (NFT 51-035)	9	15	>500	420	>500	>500
Tensile stress at break or max. (MPa) (NFT 51-035)	–	–	14	17	19	9
Biodegradation[c] (mineralization in %)	100	100	100	100	90	100
Water permeability WVTR at 25 °C ($g/m^2/day$)	172	21	177	680	330	550
Surface tension (γ) (mN/m)	50	–	51	59	56	53
γ_d (dispersive component)	37	–	41	37	43	43
γ_p (polar component)	13	–	11	22	14	11

[a] Measured by DSC.
[b] Determined on granules, before processing.
[c] After 60 days in controlled composting according to ASTM 5336.

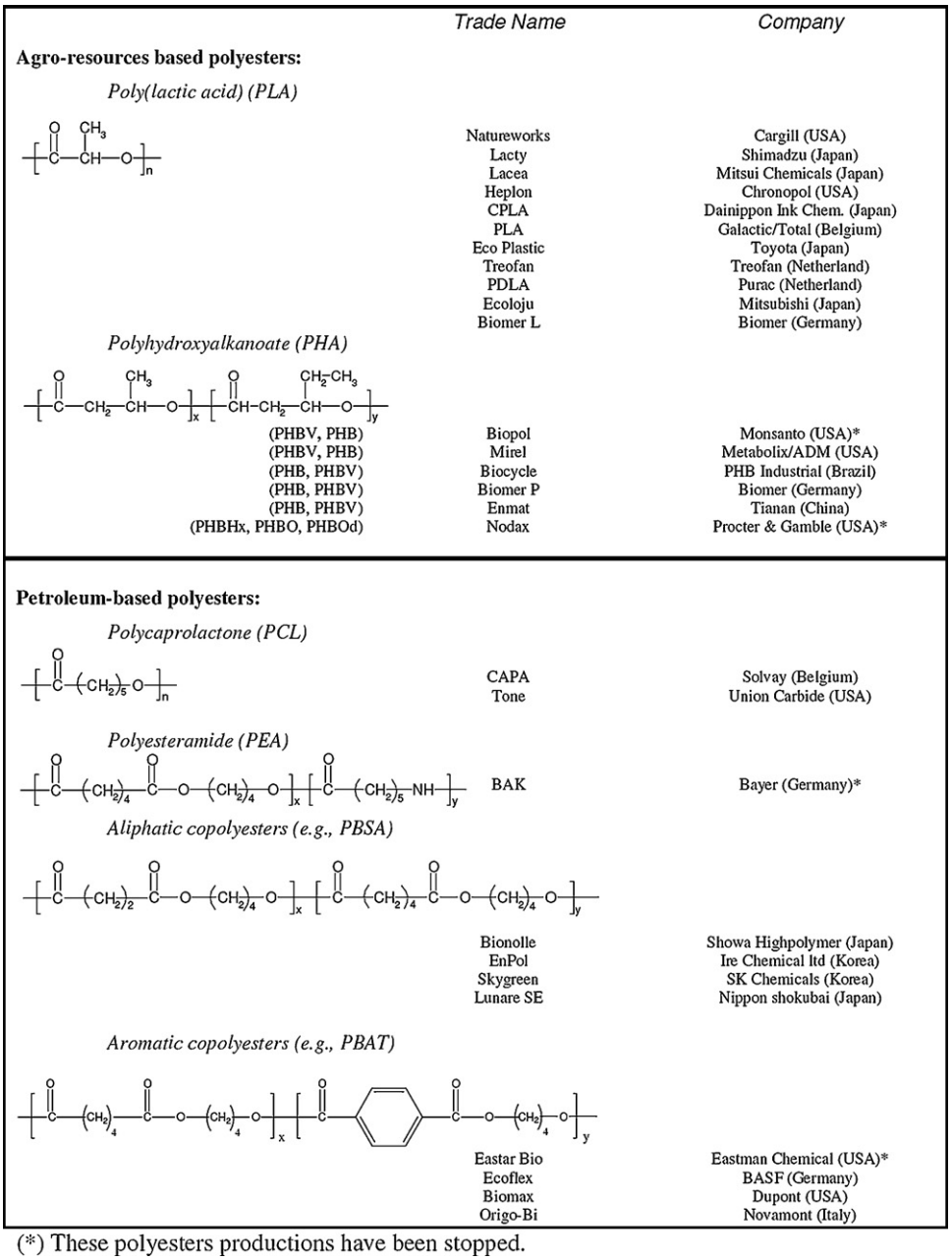

Fig. 2. Structure, trade names and suppliers of main biodegradable polyesters commercially available. Reproduced with permission from Averous [190] copyright (2004) of Marcel Dekker, Inc.

to different melting peaks [21] with a main endotherm at 152 °C for the PDLLA (see Table 1). Furthermore, PLA can be plasticized using oligomeric lactic acid *o*-LA [21], citrate ester [22] or low molecular weight polyethylene glycol PEG [21,23–25]. The effect of plasticization increases the chain mobility and then favors PLA organization and crystallization. After plasticization, we obtain a crystallinity ranging between 20% and 30%. PLA presents a medium water and oxygen permeability level [16,26] comparable to polystyrene [27]. These different properties associated with its tunability and its availability favor its actual developments in different packaging applications (trays, cups, bottles, films, etc.) [14,16,17]. McCarthy et al. [28] showed that A-PLA presents a soil degradation rate much slower compared to polybutylene succinate/adipate PBSA. PLA is presumed to be biodegradable although the role of hydrolysis vs. enzymatic depolymerization in this process remains open to debate [29]. Regarding biodegradation in compost, adequate conditions are only found in industrial units with a high temperature (above 50 °C) and a high relative humidity RH% to promote chain hydrolysis. According to Tuominen et al. [30],

PLA biodegradation does not exhibit any eco-toxicological effect.

3.1.2. Polyhydroxyalkanoates

Polyhydroxyalkanoates PHAs are naturally produced by micro-organisms from various carbon substrates as a carbon or energy reserve. A wide variety of prokaryotic organisms [31,32] accumulate PHA from 30% to 80% of their cellular dry weight. Biotechnological studies revealed that polyhydroxybutyrate homopolymer PHB is produced under balanced growth conditions when the cells become limited for an essential nutrient but are exposed to an excess of carbon [33]. Depending on the carbon substrates and the metabolism of the micro-organism, different monomers, and thus (co)polymers, could be obtained [34]. Although PHB is the main polymer of the polyhydroxyalkanoates family, different poly(hydroxybutyrate-*co*-hydroxyalkanoates) copolyesters exist such as poly(hydroxybutyrate-*co*-hydroxyvalerate) PHBV (see Fig. 2), or poly(hydroxybutyrate-*co*-hydroxyhexanoate) PHBHx, poly(hydroxybutyrate-*co*-hydroxyoctanoate) PHBO and poly(hydroxybutyrate-*co*-hydroxyoctadecanoate) PHBOd. With progress in biotechnologies, it is possible for recombinant bacteria [32], but also plants [32,35,36] to produce such polymers. However, the recovery process, i.e., the extraction and purification steps, is decisive to obtain a highly pure PHA and often explains why such polymers are still expensive. Pure synthetic PHA can be produced by the ROP from butyrolactone and other lactones [37–42]. Thus, according to the synthesis route, we obtain different structures, isotactic with random stereosequences for the bacterial copolyesters and with partially stereoregular block for the synthetic copolyesters. Recently, Monsanto has developed genetic modification of plants to make them produce small quantities of PHB [35,43,44].

PHB is a highly crystalline polyester (above 50%) with a high melting point, T_m = 173–180 °C, compared to the other biodegradable polyesters. Glass transition temperature T_g is around 5 °C. The homopolymer shows a narrow window for the processing conditions. To ease the transformation, PHB can be plasticized with citrate ester, but the PHBV copolymer is more adapted for the process. A large range of bacterial copolymer grades had been industrially produced by Monsanto under the Biopol® trade mark, with HV contents reaching 20%. The production was stopped at the end of 1999. Metabolix bought Biopol® assets in 2001. Presently, Telles™, a joint venture between Metabolix and Archer Daniels Midlands Company (ADM), has marketed the Mirel™ product as a new bio-based biodegradable plastic from corn sugar. ADM has begun to build the first plant in Clinton, Iowa (US) which will be able to produce 50,000 tons of resin per year. The startup is scheduled for late 2008 (http://www.metabolix.com).

Different small companies currently produce bacterial PHA, e.g., PHB Industrial (Brazil) produces PHB and PHBV (HV = 12%) 45% crystalline, from sugar cane molasses [45]. The Biocycle® production is planned to be 4000 tons/year in 2008 and then, to be extended to 14,000 tons/year [46]. In 2004, Procter & Gamble (US) and Kaneka Corporation (Japan) announced a joint development agreement for the completion of R&D leading to the commercialization of Nodax, a large range of polyhydroxybutyrate-*co*-hydroxyalkanoates (PHBHx, PHBO, PHBOd) [47]. Although the industrial production was planned for 2006 with a target price around 2€/kg, the production was stopped [48].

The production of PHAs is intended to replace synthetic non-degradable polymers for a wide range of applications [48]: packaging, agriculture but also medicine [34,49] since PHAs are biocompatible. Fig. 2 and Table 1 give the chemical structure and the properties of some PHBV, respectively. Material properties can be tailored by varying the HV content. An increase of the HV content induces an increase of the impact strength and a decrease of the melting temperature and glass transition [50], the crystallinity [51], the water permeability [51] and the tensile strength [52].

Besides, PHBV properties can evolve when plasticization occurs, e.g., with citrate ester (triacetin) [52,53]. The polyhydroxyalkanoates, like the PLAs, are sensitive to the processing conditions. Under extrusion, we obtain a rapid diminution of the viscosity and the molecular weight due to macromolecular chain cleavage by increasing the shear level, the temperature and/or the residential time [54]. Regarding the biodegradable behavior, the kinetic of enzymatic degradation is variable according to the crystallinity, the structure [45,55] and then, to the processing history [56]. Bacterial copolyesters biodegrade faster than homopolymers [57] and synthetic copolyesters [58].

3.2. Petroleum-based polyesters

A large number of biodegradable polyesters are based on petroleum resources, obtained chemically from synthetic monomers [11–15,17,18]. According to the chemical structures (see Fig. 2), we can distinguish (see Table 1) polycaprolactones, polyesteramides, aliphatic or aromatic copolyesters. All these polyesters are soft at room temperature.

3.2.1. Polycaprolactone

Poly(ε-caprolactone) PCL is usually obtained by ROP of ε-caprolactone in the presence of metal alkoxides (aluminium isopropoxide, tin octoate, etc.) [11,12,58]. PCL is widely used as a PVC solid plasticizer or for polyurethane applications, as polyols, but it finds also some applications based on its biodegradable character in domains such as biomedicine (e.g., drugs controlled release) and environment (e.g., soft compostable packaging). Different commercial grades are produced by Solvay (CAPA®),[1] by Union Carbide (Tone®) and by Daicel (Celgreen®). Fig. 2 and Table 1 give, respectively, the chemical structure and the properties of this polyester. PCL shows a very low T_g (−61 °C) and a low melting point (65 °C), which could be a handicap in some applications. Therefore, PCL is generally blended [29,59–61] or modified (e.g., copolymerization, crosslinking [62]). Tokiwa and Suzuki [63] have discussed the hydrolysis of PCL and biodegradation by fungi. They have shown that PCL can be easily enzymatically degraded. According to Bastioli [29], the biodegradability can be clearly claimed but the homopolymer hydrolysis rate is

[1] Solvay has recently sold this activity to Perstorp (Sweden).

very low. The presence of starch can significantly increase the biodegradation rate of PCL [59].

3.2.2. Biodegradable aliphatic polyesters

A large number of aliphatic copolyesters are biodegradable copolymers based on petroleum resources. They are obtained by the combination of diols such as 1,2-ethanediol, 1,3-propanediol or 1,4-butadenediol, and dicarboxylic acids like adipic, sebacic or succinic acid. Showa Highpolymer (Japan) has developed a large range of polybutylene succinate PBS obtained by polycondensation of 1,4-butanediol and succinic acid. Polybutylene succinate/adipate PBSA, presented in Fig. 2, is obtained by addition of adipic acid. These copolymers are commercialized under the Bionolle® trademark [17]. Table 1 shows the properties of such biopolyester. Ire Chemical (Korea) commercializes exactly the same kind of copolyesters under EnPol® trademark. Skygreen®, a product from SK Chemicals (Korea) is obtained by polycondensation of 1,2-ethanediol, 1,4-butadenediol with succinic and adipic acids [64]. Nippon Shokubai (Japan) also commercializes an aliphatic copolyester under Lunare SE® trademark. These copolyesters properties depend on the structure [65], i.e., the combination of diols and diacids used. These products biodegradability depends also on the structure. The addition of adipic acid, which decreases the crystallinity [66] tends to increase the compost biodegradation rate [67]. According to Ratto et al. [68], the biodegradation results demonstrate that although PBSA is inherently biodegradable, the addition of starch filler significantly improves the rate of degradation. Blending PBSA with non-degradable polymers such as poly(vinyl acetate) PVAc or linear low density poly(ethylene) LLDPE leads to immiscible systems whereas PBSA presents very good miscibility with poly(epichlorohydrin) PECH [69–71].

3.2.3. Aromatic copolyesters

Compared to totally aliphatic copolyesters, aromatic copolyesters are often based on terephthalic acid. Fig. 2 and Table 1 show, respectively, the chemical structure and the properties of such products (e.g., Eastar Bio® from Eastman). Besides, BASF and DuPont commercialize aromatic copolyesters under Ecoflex® [17] and Biomax® trademarks, respectively. Biomax® shows a high terephthalic acid content which modifies some properties such as the melting temperature (200 °C). But, according to Muller et al. [65], an increase of terephthalic acid content tends to decrease the degradation rate. Ecoflex® biodegradation has been analysed by Witt et al. [72]. They concluded that there is no indication for an environmental risk (eco-toxicity) when aliphatic–aromatic copolyesters of the Ecoflex®-type are introduced into composting processes.

3.2.4. Polyesteramide

Polyesteramide was industrially obtained from the statistical copolycondensation of polyamide (PA 6 or PA 6-6) monomers and adipic acid [17,73]. Bayer had developed different commercial grades under BAK® trademark but their productions stopped in 2001. Fig. 2 and Table 1 show, respectively, the chemical structure and the properties of this poly(butylene adipate-*co*-amino caproate). Table 1 shows that this polyester presents the highest polar component, and then presents good compatibility with other polar products, e.g., starchy compounds. Besides, it has the highest water permeability (see Table 1). Currently, the environmental impact of this copolymer is open to discussion. Fritz [74] had shown that, after composting, this biodegradable polyester presented a negative ecotoxicological impact but more recently, Bruns et al. [75] have infirmed these results. These authors discussed Fritz's experiments and more precisely the composting methods used.

4. Biopolyester/clay nano-biocomposites

Before discussing about the different nano-biocomposites based on the polyesters described above, it is necessary to consider some general information about the clays specific properties, as well as the different and possible elaboration routes of such materials.

4.1. Generalities

4.1.1. Clays

The clays most commonly used in the field of nanocomposites belong to the family of 2:1 layered silicates, also called 2:1 phyllosilicates (montmorillonite, saponite). Their structure consists of layers made up of two tetrahedrally coordinated silicon atoms fused to an edge-shared octahedral sheet of either aluminium or magnesium hydroxide (see Fig. 3). Each layered sheet is about 1 nm thick and its length varies from tens of nanometers to more than one micron, depending on the layered silicate. Layer stacking leads to a regular Van der Waals gap between the platelets called the interlayer or the gallery. Isomorphic substitution may occur inside the sheet since Al^{3+} can be replaced by Mg^{2+} or Fe^{2+}, and Mg^{2+} by Li^{+}. Globally negatively charged platelets are counterbalanced by alkali and alkali earth cations (Na^{+}, Ca^{2+}, etc.) located in the galleries, which increases the clay hydrophilic character. Most polymers, and particularly the biopolyesters are considered to be organophilic compounds. Thus, to obtain better affinity between the filler and the matrix, and eventually to improve final properties, the inorganic cations located inside the galleries (Na^{+}, Ca^{2+}, etc.) are generally exchanged by ammonium or phosphonium cations bearing at least one long alkyl chain, and possibly other substituted groups. The resulting clays are called organomodified layered silicates OMLS and, in the case of montmorillonite MMT, are abbreviated OMMT. By modifying the layered silicate, it is possible to compatibilize the matrix and the filler, which will affect the material nanostructure, and consequently the properties of the nanocomposites. Tables 2 and 3 present the characteristics of the main 2:1 layered silicates and commercial clays.

4.1.2. Elaboration routes

An important key factor in the nanocomposites preparation is the elaboration protocol. Nowadays, three main

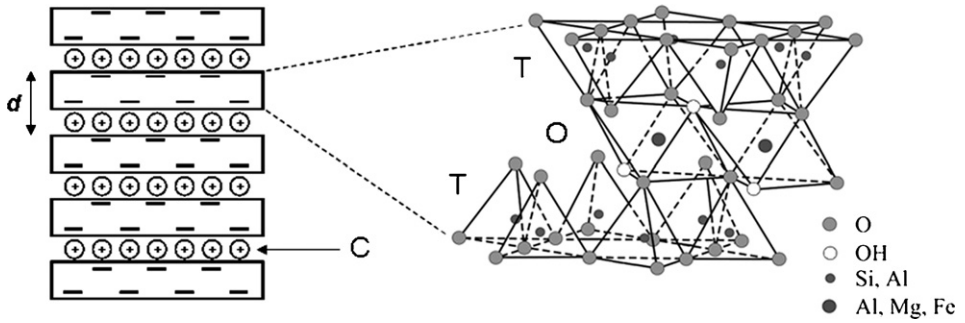

Fig. 3. 2:1 layered silicate structure (T, tetrahedral sheet; O, octahedral sheet; C, intercalated cations; *d*, interlayer distance). Reproduced with permission from Lagaly [191] copyright (1993) of Marcel Dekker.

Table 2
Structural characteristics of principal 2:1 layered silicates. Adapted and reproduced with permission from Sinha Ray et al. and Utracki et al. [192,193] copyright (2003) of Elsevier Science Ltd. and copyright (2007) of John Wiley & Sons, Ltd.

Phyllosilicates	Octahedra occupancy	Interlayer cations	CEC (meq/100 g)	Aspect ratio
Smectites				
Hectorite	Mg (3/3)	Na^+, Ca^{2+}, Mg^{2+}	120	200–300
Montmorillonite	Al (2/3)	Na^+, Ca^{2+}, Mg^{2+}	110	100–150
Saponite	Mg (3/3)	Na^+, Ca^{2+}, Mg^{2+}	86.6	50–60

methods are applied: (i) the solvent intercalation route which consists in swelling the layered silicates in a polymer solvent to promote the macromolecules diffusion in the clay interlayer spacing, (ii) the in-situ intercalation method for which the layered silicates are swollen in the monomer or monomer solution before polymerization, and (iii) the melt intercalation process which is based on polymer processing in the molten state such as extrusion. Obviously, the latter method is highly preferred in the context of sustainable development since it avoids the use of organic solvents, which are not eco-friendly and then alter the life cycle analysis LCA.

4.1.3. Nanocomposites structures

Finally, different structures of nanocomposites could be obtained:

(i) a microcomposite when the clay layers are still stacked and the polymer is not intercalated within the (O)MMT's layers due to poor polymer-clay affinity, the material thus presents phase separation;
(ii) an intercalated nanocomposite for which the polymer is partially intercalated between the silicate layers; these latter are still stacked but the interlayer spacing has increased;

Table 3
Commercial (O)MMT and their characteristics.

Commercial clays Supplier/trade name/designation		Clay type	Organomodifier type	Modifier concentration (meq/100 g)	Δw[a] (%)	*d*-spacing (Å)
Southern Clay Products (USA)						
Cloisite®Na	CNa	MMT	–	–	7	11.7
Cloisite®15A	C15A	MMT	$N^+(Me)_2(tallow)_2$	125	43	31.5
Cloisite®20A	C20A	MMT	$N^+(Me)_2(tallow)_2$	95	38	24.2
Cloisite®25A	C25A	MMT	$N^+(Me)_2(C_8)(tallow)$	95	34	18.6
Cloisite®93A	C93A	MMT	$NH^+(Me)(tallow)_2$	90	37.5	23.6
Cloisite®30B	C30B	MMT	$N^+(Me)(EtOH)_2(tallow)$	90	30	18.5
Süd-Chemie (Germany)						
Nanofil®804	N804	MMT	$N^+(Me)(EtOH)_2(tallow)$		21	18
Laviosa Chimica Mineraria (Italy)						
Dellite® LVF	LVF	MMT	–	105	4–6	9.8
Dellite® 43B	D43B	MMT	$N^+(Me)_2(CH_2\text{-}\phi)(tallow)$	95	32–35	18.6
CBC Co. (Japan)						
Somasif	MEE	SFM	$N^+(Me)(EtOH)_2(coco\ alkyl)$	120	28	
	MAE	SFM	$N^+(Me)_2(tallow)_2$	120	41	

Tallow: ~65% C_{18}; ~30% C_{16}; ~5% C_{14}.
[a] %Weight loss on ignition.

(iii) eventually, an exfoliated nanocomposite showing individual and well-dispersed clay platelets into the matrix; in this case, the layered structure does not exist anymore.

4.2. Polyesters matrices based on agro-resources

4.2.1. Poly(lactic acid)-based nano-biocomposites

PLA is a very promising material since it has good mechanical properties, thermal plasticity and biocompatibility. However, some of its properties, like flexural properties, gas permeability and heat distortion temperature, are too low for widespread applications. Therefore, many attempts were carried out to reach exfoliation state in corresponding nano-biocomposites. Various organoclays with different organomodifiers were selected and several elaboration routes were tested (see Table 4).

Ogata et al. [76] first attempted to prepare PLA-based nanocomposites by the solvent intercalation method. Unfortunately, the layered silicates were not individually well dispersed but rather formed tactoids consisting of several stacked silicate monolayers. Consequently, although the Young's modulus increased with the clay content, the increments were small compared to conventional nanocomposites. Later, Chang et al. [77,78] examined the influence of the layered silicates aspect ratio (montmorillonite, fluorinated synthetic mica), of the organomodifier ($N^+(Me)_2(C_8)$(tallow)-C25A-, hexadecylamine-C_{16}-, dodecyltrimethyl ammonium bromide-DTA) and of the clay content on the nanofiller dispersion into a PLA matrix. It was shown by X-ray diffraction XRD and transmission electron microscopy TEM that intercalated structures were obtained, leading to some improvements in mechanical and barrier properties with only small amount of fillers. Compared to neat PLA, the ultimate strength increased by about 65%, 47% and 131% in the case of PLA with 2 wt% of C25A, 4 wt% of C_{16}-MMT and C_{16}-mica, respectively. However, it appeared that the mechanical enhancement was limited to a small range of clay content (up to 4–6 wt% depending on the organomodifier). Above these clay contents, properties decreased due to layered silicates agglomeration. Considering O_2 permeability, a decrease of more than a half is observed at 10 wt% of OMMT. The initial degradation temperatures decreased linearly with an increasing OMMT amount reaching a maximum shift of 49 and 41 °C in the case of 8 wt% of C_{16}-MMT and C25A, respectively. In the case of C_{16}-mica at the same clay loading, the decrease was only of 16 °C. It was also shown that DTA-MMT presents a particular thermal behavior since the initial degradation temperature was not affected by the clay content [78].

Finally, Krikorian and Pochan [79] successfully prepared exfoliated materials with randomly distributed clay platelets via solvent intercalation in the presence of C30B. Since C30B bears a long alkyl chain and hydroxyl groups, the interactions between OH functions from the clay organomodifier and C=O moieties of the PLA backbone favored exfoliation. Therefore, the mechanical properties were improved, e.g., the storage modulus increased by 61% with 15 wt% of C30B. A complete study of the crystallization behavior of such materials was also conducted [80,81],

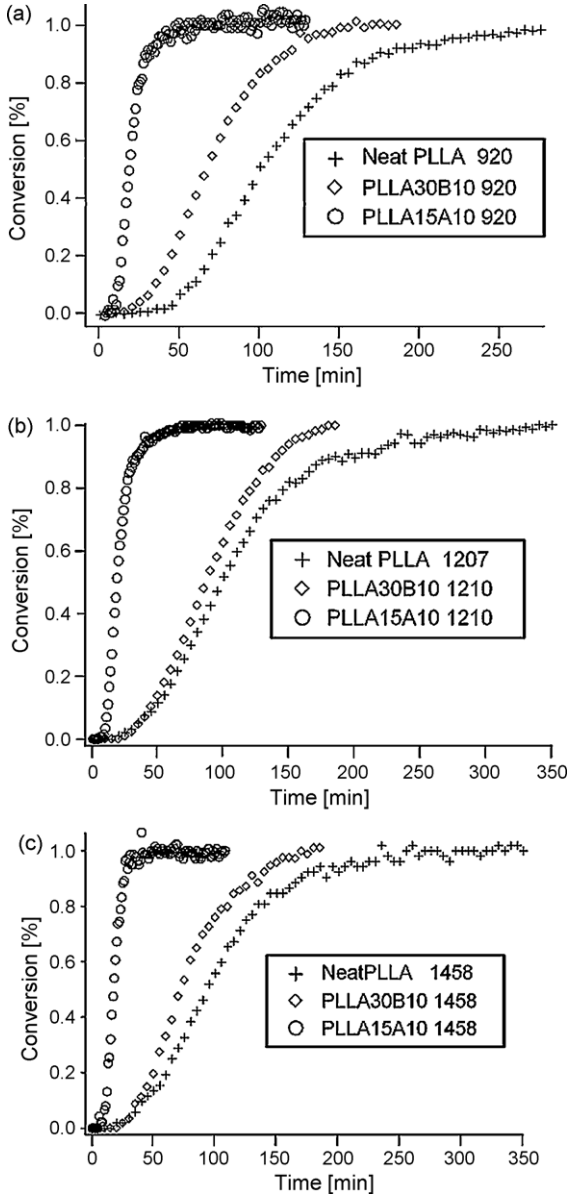

Fig. 4. FT-IR normalized peak intensities at (a) 920, (b) 1210, and (c) 1458 cm^{-1} as a function of crystallization time for neat PLLA, PLLA with 10% of C15A and PLLA with 10% of C30B. Reproduced with permission from Krikorian and Pochan [81] copyright (2005) of the American Chemical Society.

focusing on the role of intercalated or exfoliated layered silicates on the nucleation, the growth, and thus, the overall crystallinity. They demonstrated that addition of highly miscible clay leads to low spherulite nucleation, low bulk crystallization, and as a result, much lower extent of crystallinity compared to neat polymer. Moreover, from FTIR analyses, they described the mechanisms of crystallization and explained how the highly miscible clay hinders the crystal nuclei formation (see Fig. 4) [81].

Exfoliated structure of PLA-based nanocomposites was also obtained by Wu and Wu [82] using a solution mixing process. They increased the interactions between the

Table 4
Structure of the studied PLA/clay nano-biocomposites.

Process	System	Structure	Reference
Solvent intercalation	MMT-$N^+(Me)_2(C_{18})_2$/chloroform	Tactoids	[76]
	SFM-$NH_3^+(C_{16})$/dimethylacetamide MMT-$NH_3^+(C_{16})$/dimethylacetamide MMT-$N^+(Me)_3(C_{12})$/dimethylacetamide MMT-$N^+(Me)_2(C_8)$(tallow)/dimethylacetamide	Intercalated	[77,78]
	MMT-$N^+(Me)(EtOH)_2$(tallow)/dichloromethane	Exfoliated	[79]
	MMT-$N^+(Me)_3(C_{16})$ + chitosan/methylene chloride	Exfoliated	[82]
In-situ intercalation	MMT-$N^+(Me)_2(C_8)$(tallow)/triethylaluminium	Intercalated	[108,113]
	MMT-$N^+(Me)_2(C_8)$(tallow)/tin octoate	Intercalated	[113]
	MMT-$N^+(Me)(EtOH)_2$(tallow)/triethylaluminium	Exfoliated	[108,113]
	MMT-$N^+(Me)(EtOH)_2$(tallow)/tin octoate	Exfoliated	[113]
	MMT-$N^+(Me)(EtOH)_2$(tallow)/α-ω-diOH o-PEG/tin octoate	Exfoliated	[108]
Melt intercalation	MMT-$NH_3^+(C_{18})$	Intercalated-flocculated Intercalated	[88,92–94] [84,112]
	MMT-$NH_3^+(C_{18})$/o-PCL	Intercalated-flocculated	[88]
	MMT-$NH_3^+(C_{18})$/o-PEG	Intercalated	[112]
	MMT-$NH_3^+(C_{18})$/diglycerine tetraacetate	Intercalated	[112]
	MMT-$NH^+(EtOH)_2(C_{18})$ MMT-$NH^+(EtOH)_2(C_{18})$/o-PEG MMT-$NH^+(EtOH)_2(C_{18})$/diglycerine tetraacetate	Intercalated	[112]
	MMT-$N^+(Me)_3(C_{18})$	Intercalated	[86,89,92,94,97]
	MMT-$N^+(Me)_2(C_{18})_2$	Intercalated-flocculated Intercalated (tactoids of 5–7 layers)	[94,95] [96,97]
	MMT-$N^+(Me)_2(C_{18})_2$/PCL	Intercalated	[105]
	MMT-$N^+(Me)_2(C_{18})_2$/o-PEG	Intercalated	[111]
	MMT-$N^+(Me)_2(C_{18})_2$/PEG	Intercalated	[111]
	MMT-$N^+(Me)_2(CH_2\text{-}\phi)(C_{18})$/o-PEG	Intercalated	[111]
	MMT-$N^+(Me)_2(CH_2\text{-}\phi)(C_{18})$/PEG	Intercalated	[111]
	MMT-$N^+(Me)_2(C_8)$(tallow)	Intercalated	[107]
	MMT-$N^+(Me)_2(C_8)$(tallow)/PBS	Intercalated	[102,103]
	MMT-$N^+(Me)_2(C_8)$(tallow)/o-PEG	Intercalated	[106,107,109,110]
	GPS-g-MMT-$N^+(Me)_2(C_8)$(tallow)/PBS	Exfoliated or Intercalated/exfoliated	[102,103]
	MMT-$N^+(Me)_2$(tallow)$_2$	Intercalated	[98]
	MMT-$N^+(Me)_2$(tallow)$_2$/o-PEG	Intercalated	[106,109,110]
	MMT-$N^+(Me)(ButOH)_2(C_{18})$	Flocculated (tactoids of 1–3 layers)	[96,97]
	MMT-$N^+(Me)(EtOH)_2$(tallow)	Intercalated	[98]
	MMT-$N^+(Me)(EtOH)_2$(tallow)/o-PEG	Intercalated	[106,109,110]
	MMT-$P^+(But)_3(C_{16})$	Intercalated	[85]
	Smectite-$P^+(But)_3(C_8)$	Not intercalated	[85]
	Smectite-$P^+(But)_3(C_{12})$	Intercalated	[85]
	Smectite-$P^+(But)_3(C_{16})$	Intercalated and low ordered	[85]
	Smectite-$P^+(Me)(\phi)_3$	Not intercalated	[85]
	Mica-$P^+(But)_3(C_{16})$	Intercalated and well ordered	[85]
	SFM-$N^+(Me)(EtOH)_2$(coco alkyl)	Intercalated/exfoliated Intercalated-flocculated	[87] [90,92,94]
	SFM-$N^+(Me)_2$(tallow)$_2$	Intercalated	[84]
	SAP-$P^+(But)_3(C_{16})$	Exfoliated	[92,94]
Masterbatch	MMT-$N^+(Me)_2(EtOH)_2$/PLLA/triethylaluminium + PDLLA MMT-$N^+(Me)_2(EtOH)_2$/PLLA/o-PEG/triethylaluminium + PDLLA	Intercalated/exfoliated	[108]
	MMT-$N^+(Me)_2(C_8)$(tallow)/PLLA + PDLLA	N.D.	[104]

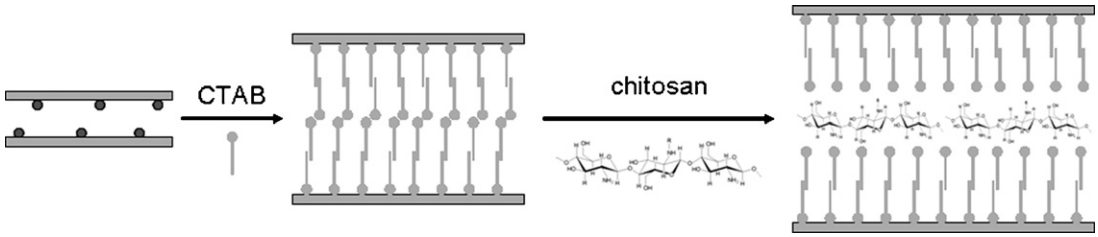

Fig. 5. Schematic drawing of montmorillonite organomodification by CTAB and chitosan. Reproduced with permission from Wu and Wu [82] copyright (2006) of Elsevier Science Ltd.

filler and the matrix by treating the montmorillonite with *n*-hexadecyl trimethylammonium bromide (CTAB) cations and then modified it with chitosan, a biodegradable and biocompatible polymer (see Fig. 5).

The elaboration of PLA/clay nano-biocomposites by melt intercalation is also widely described in the literature [83–98], leading to various materials structures. Okamoto and his group at Toyota Technological Institute (Nagoya, Japan) tested a lot of PLA-based systems differing from the OMLS in the aspect ratio of the inorganic platelets, the nature of the organomodifier, and the clay content [85–95]. Depending on these parameters, intercalated, intercalated-and-flocculated, nearly exfoliated, or the coexistence of intercalated and exfoliated states were obtained. They even proposed an interpretation of the nanocomposites structure related to the aspect ratio and the organomodifier chain lengths [85]. Regarding the aspect ratio, it was demonstrated that the smaller the silicate layers size, the lower the physical jamming, restricting the conformation of organomodifier alkyl chains, and thus, the lower the coherency of the organoclay (see Fig. 6). Due to a nicely stacked structure of organomodified mica, the polymer chains can hardly penetrate up to the core of the silicate layers, contrary to smaller size of silicate layers such as smectite and MMT (see Fig. 6). The effect of organomodifiers organization in the interlayer space was also examined considering an interdigitated layer structure of the surfactants [99].

Flocculated structures were further studied by Nam et al. [96,97] using bis(4-hydroxy butyl) methyl

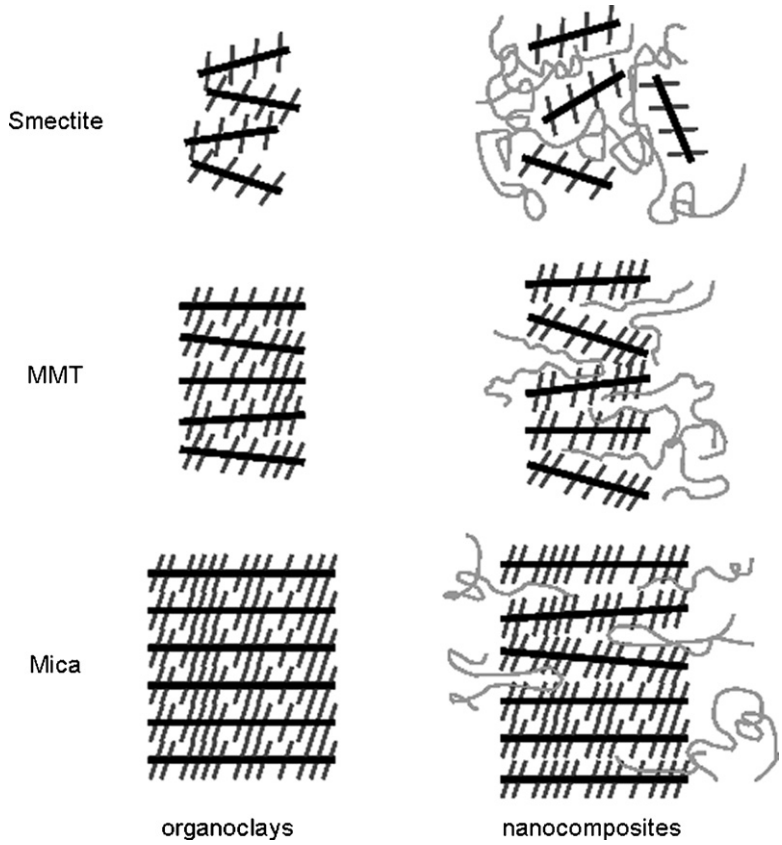

Fig. 6. Structure of organoclays and the corresponding nanocomposites depending on the type of layered silicates. Reproduced with permission from Maiti et al. [85] copyright (2002) of the American Chemical Society.

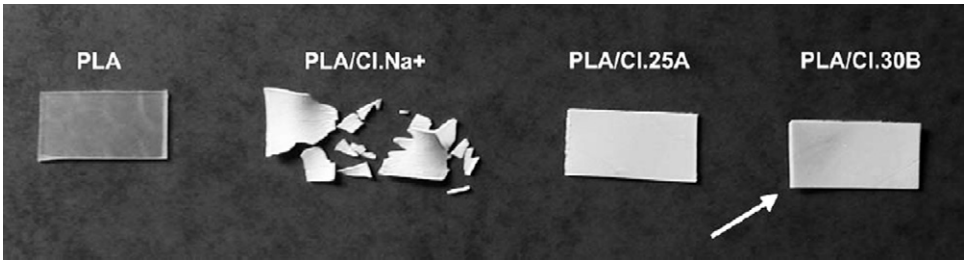

Fig. 7. Visual aspect of PLA matrix, microcomposite based on CNa and nanocomposites based on C25A and C30B, respectively, after five and a half months of hydrolysis (the white arrow points the curvature of the sample). Reproduced with permission from Paul et al. [98] copyright (2005) of Elsevier Science Ltd.

octadecyl ammonium modified montmorillonite (MMT-$N^+(Me)(ButOH)_2(C_{18})$). From polarized optical microscopy POM, TEM and particularly FT-IR, they showed that the formation of such nanocomposite structures could be due to hydrogen bonding among the hydroxyl groups of the surfactant, those of platelets edges and those of both ends of the PLA chains.

As a consequence of the nanostructure, and despite of the fact that incomplete exfoliation was obtained by melt intercalation, all these nano-biocomposites exhibited dramatic enhancements of various materials properties. These improvements included mechanical and flexural properties, heat distortion temperature, and O_2 gas permeability. However, it has to be noticed that the increments strongly depend on the structure of the nanocomposites. A particular study of the crystallization behavior of the well-ordered intercalated PLA/octadecylammonium OMMT (MMT-$NH_3^+(C_{18})$) nanocomposite revealed a spherulite size decrease and an overall crystallization rate enhancement compared to neat PLA [100]. This was attributed to the clay nucleating effect. Furthermore, since the compostability is controlled by the crystallinity, the molecular weight and the (OM)LS dispersion, it was enhanced by the incorporation of layered silicates [92,101]. Paul et al. [98] studied the hydrolytic degradation in such materials and concluded that the more hydrophilic the filler, the more pronounced the degradation. This was expressed by increasing opacity and shape modification before fragmentation (see Fig. 7).

Eventually, the addition of the most appropriate OMLS could also enhance the properties of polymers blends as described by Chen et al. [102,103] who used a specific organoclay to compatibilize an immiscible PLLA/PBS blend. They introduced epoxy groups to C25A by treating the clay with (glycidoxypropyl)trimethoxy silane (GPS) to produce a twice-functionalized organoclay TFC (see Fig. 8). Reacting with epoxy groups located on the clay surface, the biopolyesters tend to delaminate the platelets (see Fig. 9). However, since TFC was highly compatible with PLLA rather than PBS, at small TFC content, the clays are located almost exclusively in the PLLA phase and are fully exfoliated. At higher TFC content, the clay layers were dispersed in both PBS and PLLA phases with intercalated/exfoliated coexisting morphology. The domains size of the dispersed PBS phase decreased sharply since the platelets hinders the PBS domains coalescence. The addition of TFC to the PLLA/PBS blend not only improved the tensile modulus but also the elongation at break, while the incorporation of C25A to the same polymer blend increased the tensile modulus but at the cost of the elongation at break. The thermal stability of these materials, in terms of onset temperature and activation energy of degradation was also enhanced [103].

Therefore, by a judicious choice of the OMLS, it is possible to tune the material properties [92]. Furthermore, the process could also play a key role in the final nano-biocomposites structure and properties. For example, Lewitus et al. [104] prepared nano-biocomposites

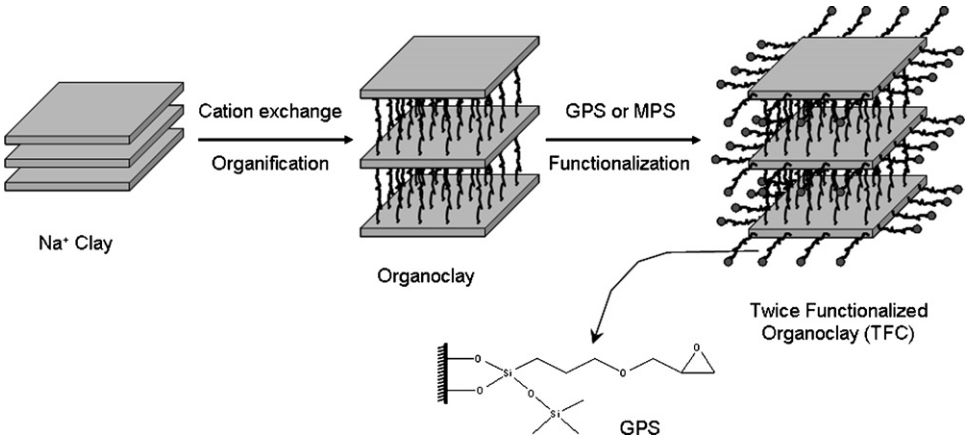

Fig. 8. Schematic drawing of the twice-functionalized organoclay (TFC) preparation. Reproduced with permission from Chen and Yoon [182] copyright (2005) of the Society of Chemical Industry.

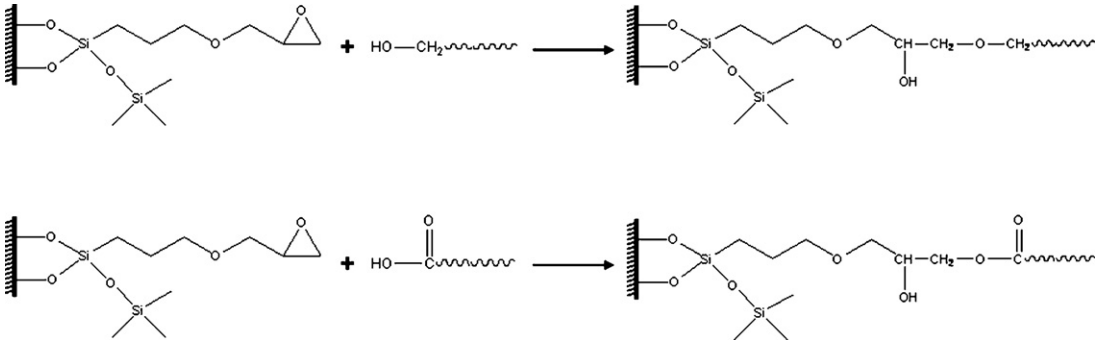

Fig. 9. Reaction between the epoxy groups in TFC and the functional end-groups of the polyesters Reproduced with permission from Chen and Yoon [103] copyright (2005) of Elsevier Science Ltd.

from PLLA-based masterbatches which were dispersed into different matrices (PLLA, PDLLA, PBAT). Compared to neat PLLA, the corresponding nano-biocomposites demonstrated enhanced film properties, showing a potential extend to film applications as, e.g., compostable packaging. The most significant improvements were obtained when the PLLA-nanoclays masterbatches were dispersed into the same PLLA matrix. In this case, the incorporation of 5 wt% of clay increased the tensile modulus and the elongation at break of PLLA by 36% and 48%, respectively, while the tensile strength did not change significantly. Authors attributed this toughening effect to molecular interactions between nanoclays and PLA but also to a high degree of exfoliation. Unfortunately, without complementary characterizations of these systems, these results could not be confirmed. Regarding the thermal properties, it was proved that clays acted as nucleating agent since the cold crystallization temperature was decreased by 15 °C.

The melt intercalation process allows incorporation of additives such as compatibilizers and plasticizers. The addition of oligo-PCL [88] (o-PCL) or PCL [105] to PLA-clay systems had not a beneficial effect on the interlayer spacing. However, the o-PCL, used as compatibilizer, induced a flocculated state due to hydroxylated edge–edge interactions of layered silicates leading to great enhancement of mechanical properties. Hasook et al. [105] also obtained reinforced materials properties when adding 5 wt% of PCL with short chain length (<40,000).

Some authors were also interested in developing plasticized PLA-based nanocomposites to reduce the brittleness and to improve the flowability during the process. Thus, PLA plasticized with PEG [106–111] or diglycerine tetraacetate [112] was melt compounded with different organoclays leading to intercalated structures. Paul et al. [106] and Pluta et al. [109] showed that there is a real competition between PEG and PLA for the intercalation into the clay interlayer. Tanoue et al. [111] also studied the structure of such materials using PEG with different molecular weight. With a certain type of organoclay, i.e., dimethyl distearyl ammonium modified MMT (MMT-$N^+(Me)_2(C_{18})_2$), these authors demonstrated that the interlayer distance depends on the PEG chain length. Besides, they pointed out that addition of PEG affects the dispersion of clay in the PLA matrix resulting in more aggregated structures. Mechanical properties can be improved [111,112] and crystallization enhanced [107,112] by selecting the right organoclay, plasticizer nature, content and chain length. Nevertheless, Pluta et al. [110] demonstrated that although the dispersed nanoclays can slow down the phase separation, particularly in the case of better PLA-clay affinity (i.e., C20A and C30B), PEG can diffuse toward the surface. Therefore, Paul et al. [108] settled a protocol consisting in the in-situ polymerization of lactide from end-hydroxylated PEG in presence of C30B with tin octoate ($Sn(Oct)_2$) as an activator/initiator. This polymerization method, called the "coordination-insertion" method, leads to PLA chains grafted onto the clay surface via the hydroxylated ammonium organomodifier and to PLA-b-PEG-b-PLA triblock copolymer intercalated into the clay gallery. The plasticizing effect is ensured by the PEG sequence of the triblock without phase separation. More generally, this mechanism allows complete exfoliation by ROP of lactide after adequate activation [113]. In the particular case of activation reaction with triethylaluminium ($AlEt_3$) [108], the polymerization is initiated by the hydroxyl groups of the OMMT organomodifier (see Fig. 10). The as-obtained PLA/OMMT nanocomposites presented enhanced thermal properties since the temperature corresponding to 50% of weight loss is shifted by ~30 °C towards higher temperature. The crystallinity was also affected since the mobility of the resulting grafted chains was restricted while T_g and T_m were not influenced by the clay [108].

Recent publications reported works on more applicative researches since they deal with PLA-based nanocomposites for preparation of porous ceramic materials [114] or for scaffolds as supports for tissue regeneration [115,116]. Foams were also elaborated from PLA/OMMT nanocomposites with the aim of obtaining high cell density and a controlled morphology varying from microcellular to nanocellular structures [117].

To conclude, the literature shows many publications on PLA-based nano-biocomposites, wherein several answers and strategies are proposed to improve the material properties since PLA is commercially and largely available.

4.2.2. Polyhydroxyalkanoates-based nano-biocomposites

Some drawbacks of PHAs, such as brittleness and poor thermal stability restrict their developments and uses. Therefore, nano-biocomposites appear as a possi-

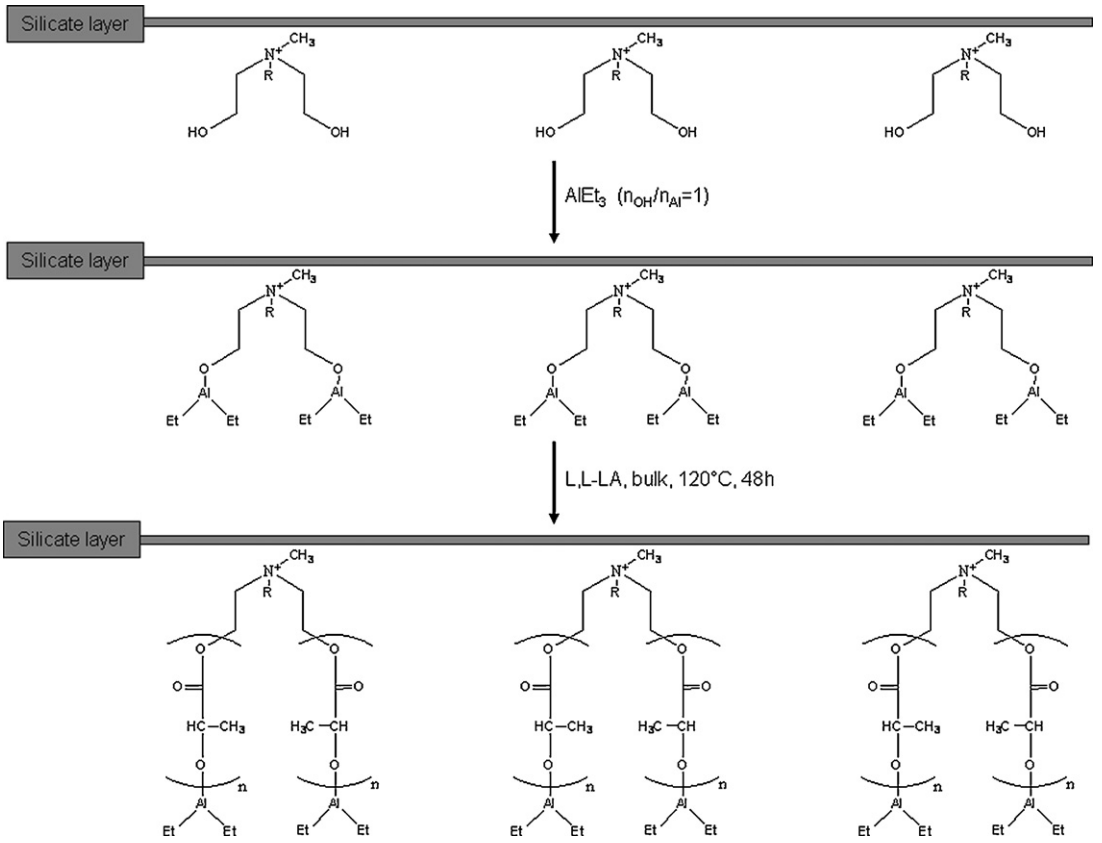

Fig. 10. Schematic representation of the L,L-lactide polymerization performed in-situ from C30B using triethylaluminium ($AlEt_3$) as initiator precursor (R stands for tallow chain). Reproduced with permission from Paul et al. [108] copyright (2005) of Wiley-VCH.

ble answer to overcome these problems and to improve different properties as, e.g., permeability. The studied PHA-based nano-biocomposites are summarized in Table 5 and described below.

First, Maiti et al. [118] prepared PHB-based nanocomposites by melt extrusion. PHB was then reinforced using organomodified fluoromicas or montmorillonite containing 2 wt% and up to 4 wt% of clay, respectively. MEE and MAE fluoromicas (see Table 3) as well as OMMT modified with octadecylammonium (MMT-$NH_3^+(C_{18})$) were selected. XRD and TEM revealed well-ordered intercalated nanocomposites with decreasing *d*-spacing with clay content increases. Dynamic mechanical analyses revealed a better reinforcing effect of fluoromica compared to montmorillonite. The storage modulus *E′* increased with clay content reaching an increment of 35% with 3.6 wt% of MMT-C_{18}, +33% and +40% with 2 wt% of MAE and MEE, respectively. These authors explained this behavior by an enhanced degradation in presence of OMMT, due to the presence of Al Lewis acid sites in the inorganic layers which catalyze the ester linkages hydrolysis. This phenomenon does not occur in the case of fluoromica since they are based on magnesium. Nevertheless, recently, Hablot et al. [119] reported that PHB enhanced degradation can also be caused by decomposition products of clay organomodifiers which have a catalyzing effect on the thermal or thermo-mechanical degradation. Eventually, the biodegradation studies also highlighted the difference between montmorillonite and fluoromicas since the initial degradation rate of PHB with MMT-$NH_3^+(C_{18})$ was higher than with fluo-

Table 5
Structure of the studied PHA/clay nano-biocomposites.

PHA	Process	System	Structure	Reference
PHB	Solvent intercalation	MMT-$N^+(Me)_2(C_8)$(tallow)/chloroform	Intercalated	[120]
	Melt intercalation	MMT-$NH_3^+(C_{18})$	Intercalated	[84,118]
		MMT-$N^+(Me)(EtOH)_2$(tallow)/MA-g-PHB	Intercalated, well delaminated	[126]
		SFM-$N^+(Me)(EtOH)_2$(coco alkyl)	Intercalated	[84,118]
		SFM-$N^+(Me)_2$(tallow)$_2$	Intercalated	[84,118]
PHBV	Solvent intercalation	MMT-$N^+(Me)_3(C_{16})$/chloroform	Intercalated	[122–124]
	Melt intercalation	MMT-$N^+(Me)(EtOH)_2$(tallow)	Intercalated, nanodispersion	[121]

romicas [118]. In this case, the degradation rates have been considerably reduced and even suppressed with MEE.

A similar study on PHB-based nanocomposites was carried out by Lim et al. [120]. Nevertheless, they used solvent intercalation route to obtain PHB/C25A with 3, 6 and 9 wt% of clay content. XRD data led to the conclusion of intercalated structures, the interlayer distance reaching 35 Å, but no dependence on clay content was observed. These results were confirmed by FTIR analyses showing that two distinct different phases coexisted. These structural observations were completed by the thermal stability investigation. TGA results indicated an increase of the onset temperature of weight loss and a decrease of the degradation rate with 3 wt% of C25A. This was attributed to the nanoscale OMMT layers dispersion decreasing the diffusion of volatile decomposition products. At higher clay contents (>6 wt%), although the onset of thermal degradation did not increase because of the organomodifier's thermal sensitivity, the nanocomposites degradation rates decreased due to restricted thermal motion of the polymer chains in the OMMT interlayer.

Scientists were also interested in the development of PHBV-based nanocomposites since the PHBV presents better properties than PHB and better processability. In 2003, Choi et al. [121] described the microstructure as well as the thermal and mechanical properties of PHBV/C30B nanocomposites with low clay content. These materials were prepared by melt intercalation using a Brabender mixer. XRD and TEM clearly confirmed that intercalated nanostructures were obtained. Such structures were formed thanks to the strong hydrogen bond interactions between PHBV and the hydroxyl groups of the C30B organomodifier. They demonstrated that the nanodispersed organoclay acted as a nucleating agent, increasing the temperature and rate of PHBV crystallization. Moreover, the DSC thermograms revealed that the crystallite size was reduced in the presence of nanodispersed layers since the PHBV melting temperature are shifted to lower temperatures. Nanocomposites thermal stabilities were also studied. Thermogravimetric analyses revealed that the temperature corresponding to 3% of weight loss increased with C30B content (+10 °C with 3 wt% of filler). They explained these trends by the nanodispersion of the silicate layers into the matrix and thus concluded that the well-dispersed and layered structure accounts for an efficient barrier to the permeation of oxygen and combustion gas. Eventually, the mechanical properties showed that clays can also act as an effective reinforcing agent since the Young's modulus significantly increases from 480 to more than 790 MPa due to strong hydrogen bonding between PHBV and C30B.

Wang et al. [122] and Zhang and co-workers [123,124] have investigated the structure and the properties of PHBV/OMMT nanocomposites. They synthesized PHBV with 3 and 6.6 mol% of HV units as well as organomodified MMT via cationic exchange in an aqueous solution with hexadecyl-trimethylammonium bromide (MMT-$N^+(Me)_3(C_{16})$). Nanocomposites were prepared by the solution intercalation method, adding 1, 3, 5 or 10 wt% OMMT to a chloroform solution of PHBV and then exposing the resulting dispersions to an ultra-sonication treatment. These conditions led to intercalated structures, as shown by XRD, but clay aggregation occurred when increasing the clay content to 10 wt%.

A detailed study of the PHBV/OMMT crystallization behavior was achieved. It was shown that OMMT acted as a nucleating agent in the PHBV matrix, which increased the nucleation and the overall crystallization rate, leading to more perfect PHBV crystals [123]. With increasing amount of OMMT, the predominant crystallization mechanism of PHBV was shifted from the growth of crystals to the formation of crystalline nuclei. The nucleation effect of the organophilic clay decreased with the clay content increase. Wang et al. [122] postulated that the nanoscaled OMMT layers affect the crystallization in two opposite ways. On one hand, a small part of OMMT can increase the crystalline nuclei thus causing a more rapid crystallization rate. On the other hand, owing to the interaction of OMMT layers with PHBV chains, most of the OMMT layers restrict the motion of the PHBV chains. Therefore, the crystallization rate increased whereas the relative degree of crystallinity decreased with increasing amount of clay in the PHBV/OMMT nanocomposites. Furthermore, the PHBV processing behavior could be improved with OMMT-based nanocomposites since the processing temperature range enlarged by lowering melting temperature with the increasing clay content. The tensile properties of the corresponding materials were improved by incorporation of 3 wt% of clay [124]. Above this clay content, aggregation of clay occurred and tensile strength and strain at break decrease. Dynamic mechanical analysis, through the study of the modulus and the T_α relaxation temperature (see Fig. 11), revealed that the interface was maximized because of the nanometer size, which restricts segmental motion near the organic-inorganic interface. Thus, it confirmed that intercalated nanocomposites were formed. Eventually, the biodegradability of these nanocomposites systems in soil suspension decreased with increasing OMMT. This was related to the interactions between PHBV and OMMT, but also to water permeability, the degree of crystallinity, and the anti-microbial property of OMMT.

Eventually, Misra et al. developed a novel solvent-free method to prepare PHB functionalized by maleic anhydride (MA-g-PHB) [125]. The functionalization was successfully achieved by free radical grafting of maleic anhydride using a peroxide initiator by reactive extrusion processing. Then, they have mixed MA-g-PHB with C30B to make the organomodifier hydroxyl functions react with the MA [126]. Although, the *d*-spacing was comparable to PHB/C30B prepared by melt blending, the decrease in intensity of XRD signals and TEM images showed that more delaminated platelets were obtained.

To conclude, most of the articles reported the preparation of PHA-based nanocomposite by solvent intercalation, and whatever the elaboration route, full exfoliation state was neither obtained nor clearly demonstrated.

4.3. Petroleum-based polyesters

4.3.1. Polycaprolactone-based nano-biocomposites

PCL-based nanocomposite was the first studied nano-biocomposite. In the early 1990s, Giannelis' group from

Table 6
Structure of the studied PCL/clay nano-biocomposites.

Process	System	Structure	Reference
Solvent intercalation	MMT-$N^+(Me)_2(C_{18})_2$/chloroform	Slightly intercalated	[164]
Melt intercalation	MMT-$N^+(Me)_2(C_{18})_2$	Intercalated	[140]
	MMT-$N^+(Me)_2(C_8)$(tallow)	Intercalated	[135,145,159]
	MMT-$NH_3^+(C_{11}COOH)$	Microcomposite	[135]
	MMT-$N^+(Me)(EtOH)_2$(tallow)	Intercalated/exfoliated	[135,145,159]
		Exfoliated	[148,149]
	Smectite-$P^+(But)_3(C_8)$/o-PCL	Intercalated	[158]
	Smectite-$P^+(But)_3(C_{12})$-/o-PCL	Intercalated	[158]
	Smectite-$P^+(But)_3(C_{16})$/o-PCL	Intercalated	[158]
	Smectite-$P^+(Me)(\phi)_3$/o-PCL	Intercalated	[158]
	SFM-$P^+(But)_3(C_{16})$/o-PCL	Intercalated	[158]
	Hectorite-$P^+(But)_3(C_{16})$/o-PCL	Intercalated, almost exfoliated	[158]
Masterbatch	MMT-Na-g-PCL + PCL	Intercalated	[150]
	MMT-$N^+(Me)_2(C_8)$(tallow)-g-PCL + PCL	Intercalated	[150]
	MMT-$N^+(Me)(EtOH)_2$(tallow)-g-PCL + PCL	Intercalated	[150]
	MMT/dibutylamine terminated o-CL + PCL	Intercalated (low o-CL chain length) Intercalated/exfoliated (high o-CL chain length)	[151]
In-situ intercalation	Fluorohectorite-Cr^{3+}	Intercalated	[128]
	MMT-$NH_3^+(C_{18})$	Intercalated	[140]
	MMT-$NH_3^+(C_{11}COOH)$	Exfoliated	[127,129,132–134]
		Intercalated	[127,129,132–135,140]
	MMT-$N^+(Me)_2(C_{18})_2$	Microcomposite	[127,140]
	MMT-$N^+(Me)_3(C_{16})$	Intercalated	[131]
	MMT-$N^+(Me)_2(C_8)$(tallow)	Microcomposite	[140]
	MMT-$N^+(Me)(EtOH)_2$(tallow)	Exfoliated	[140]
	MMT/water	Slightly intercalated	[130]
	MMT-Na/tin octoate	Intercalated	[135,140]
	MMT-Na/dibutyltin dimethoxide	Intercalated	[140]
	MMT-$NH_3^+(C_{18})$/tin octoate or dibutyltin dimethoxide	Intercalated	[135,140]
	MMT-$NH_3^+(C_{11}COOH)$/tin octoate or dibutyltin dimethoxide	Intercalated	[135,140]
	MMT-$N^+(Me)_2(C_{18})_2$/tin octoate or dibutyltin dimethoxide	Intercalated	[135,140]
	MMT-$N^+(Et)_2(CH_2CHOHCH_3)(C_{18})$/tin octoate	Exfoliated or Intercalated/exfoliated	[136]
	MMT-$N^+(Me)_2(C_8)$(tallow)/tin octoate	Intercalated	[135,140,141]
	MMT-$N^+(Me)_2(C_8)$(tallow)/dibutyltin dimethoxide	Intercalated	[135–137,140,159]
	MMT-$N^+(Me)(EtOH)_2$(tallow)/tin octoate	Exfoliated	[135,137,140,142,159]
	MMT-$N^+(Me)(EtOH)_2$(tallow)/dibutyltin dimethoxide	Exfoliated	[135,140,141]
	MMT-$[N^+(Me)_2(EtOH)(C_{16})]_x[N^+(Me)_3(C_{16})]_y$/Tin (II) or Tin (IV) or Al(III) alkoxide	Exfoliated or Intercalated/exfoliated	[138,139]
	MMT-$[N^+(Me)_2(EtOH)(C_{16})]_x[N^+(Me)_3(C_{16})]_y$/triethylaluminium/toluene	Exfoliated	[143]
	SAP-$N^+(Me)_3(C_{16})$/dibutyltin dimethoxide	Intercalated	[162,163]
	SAP-$N^+(Me)_2(EtOH)(C_{16})$/dibutyltin dimethoxide		
	SAP-$N^+(Me)(EtOH)_2(C_{16})$/dibutyltin dimethoxide		
	SAP-$P^+(Me)_3(C_{16})$/dibutyltin dimethoxide		
	LAP-$N^+(Me)_3(C_{16})$/dibutyltin dimethoxide		
	LAP-$N^+(Me)_2(EtOH)(C_{16})$/dibutyltin dimethoxide		
	LAP-$N^+(Me)(EtOH)_2(C_{16})$/dibutyltin dimethoxide		
	LAP-$P^+(Me)_3(C_{16})$/dibutyltin dimethoxide		
	SAP-$P^+(Me)_3(C_{14})$/dibutyltin dimethoxyde	Intercalated	[163]
	SAP-$P^+(Me)_3(C_{12})$/dibutyltin dimethoxyde		

Cornell University (Ithaca, New York, USA) started to work on the elaboration of PCL-based nanocomposite by intercalative polymerization [127–129]. Their work was motivated by previous studies involving polymerization of ε-caprolactam in the presence of layered silicates, which suggested that lactone ROP can be catalyzed by layered silicates. Then, they decided to investigate the intercalation and polymerization of ε-caprolactone within the gallery of layered silicates. The very first PCL-based nanocomposite prepared was based on fluorohectorite, a mica-type layered silicate [128] (see Table 6). The ROP of ε-caprolactone (ε-CL) was activated by the surface of the Cr^{3+}-exchanged fluorohectorite. Indeed, the type of interlayer cations (e.g., Cr^{3+}, Cu^{2+}, Co^{2+}, Na^+) is impor-

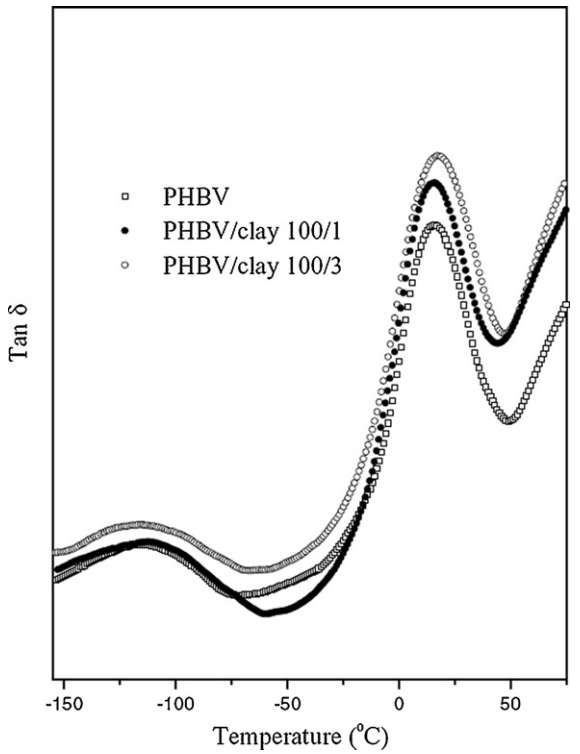

Fig. 11. Tan δ of neat PHBV and PHBV/clay nanocomposites with respectively 1 and 3 wt% of MMT-$N^+(Me)_3(C_{16})$. Reproduced with permission from Chen et al. [124] copyright (2002) of Kluwer Academic Publishers.

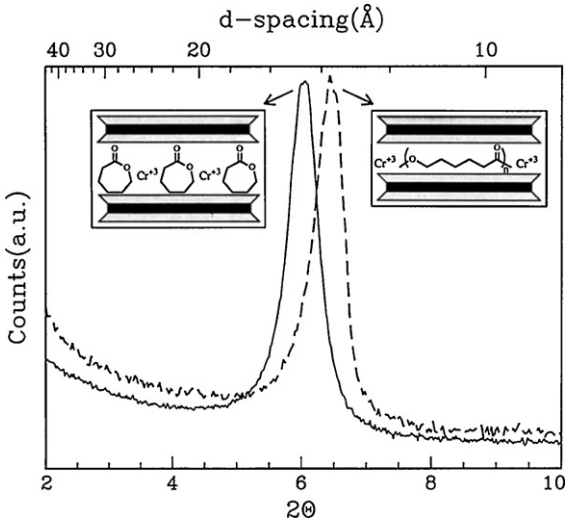

Fig. 12. XRD patterns of PCL nanocomposite before (solid lines) and after (dashed lines) polymerization. Reproduced with permission from Messersmith and Giannelis [128] copyright (1993) of the American Chemical Society.

tant in achieving polymerization since it proceeds through cleavage of the acyl-oxygen bond catalyzed by the interlayer Cr^{3+} ions which present a more acidic character than mono- and divalent cations. The polymer–clay chemical interactions at the interface was proved to be strong and the intercalation of the polymer irreversible. However, authors could also observe the decrease of *d*-spacing after polymerization. They attributed this phenomenon to a change in the intercalated molecules organization from the monomer to the polymer (see Fig. 12). Similar results were also obtained later by Kiersnowski et al. [130] who prepared the PCL-based composites by in-situ polymerization catalyzed by water. Afterwards, Messersmith and Giannelis [127] attempted to prepare PCL-based nanocomposites by in-situ polymerization thermally activated and initiated by organic acid. This one constituted the OMMT organomodifier, namely the protonated form of 12-aminododecanoic acid ($NH_3^+(C_{11}COOH)$), which was thus present on the clay surface and initiated the ROP by a nucleophilic attack on the ε-caprolactone carbonyl. The resulting PCL was therefore ionically bound to the silicate layers through the protonated amine chain end. XRD results suggested that individual silicate layers were dispersed in the matrix. On the contrary, OMMT layers organomodified with a less polar ammonium (dimethyl dioctadecyl-$N^+(Me)_2(C_{18})_2$- [127] or hexadecyltrimethyl-$N^+(Me)_3(C_{16})$- [131] ammonium) showed no dispersion in CL or PCL. Subsequently, the interactions occurring at the interface of a PCL/OMMT exfoliated nanocomposite were investigated [132,133] and the crystallinity, the permeability and the rheological behavior were examined [127,129,132,134]. Both, the crystallinity and the crystallite size decreased because of the dispersed silicate layers that represent physical barriers, and hinder PCL crystal growth. The dispersion of high aspect ratio platelets also reduced the water permeability, nearly by an order of magnitude at 4.8 vol% silicate [127]. Tortora et al. [134] who examined the water and dichloromethane permeability, assumed that the diffusion path of the polar water molecules is slowed down compared to dichloromethane vapor, not only because of the physical barrier of the clay layers, but also because of the hydrophilic character of the platelets. Eventually, the linear viscoelastic behavior of the nanocomposites with various OMMT contents was examined. A "pseudo solid-like" behavior was clearly seen at silicate loading greater than 3 wt% suggesting that domains were formed wherein some long-range order was preserved and the silicate layers were oriented in some direction. Furthermore, the non-terminal effect was more pronounced with increasing clay content. These long-range order and domain structures were hence likely to become better defined when the mean distance between the layers becomes less than the lateral dimensions of the silicate layers and thus forcing some preferential orientation between the layers.

Dubois' group (Mons, Belgium) has worked on PCL nanocomposites. They were interested in the in-situ ROP of ε-CL and in the melt intercalation route. They demonstrated that the formation of PCL-based nanocomposites depends not only on the ammonium cation and related functionality, but also on the elaboration route. Contrary to Messersmith and Giannelis [127,128], PCL-based nanocomposites were prepared by in-situ ROP according to a "coordination-insertion" mechanism [135–141] (see Fig. 13), as for PLA [108,113]. This reaction consists in swelling the OMMT organomodified by alkylammo-

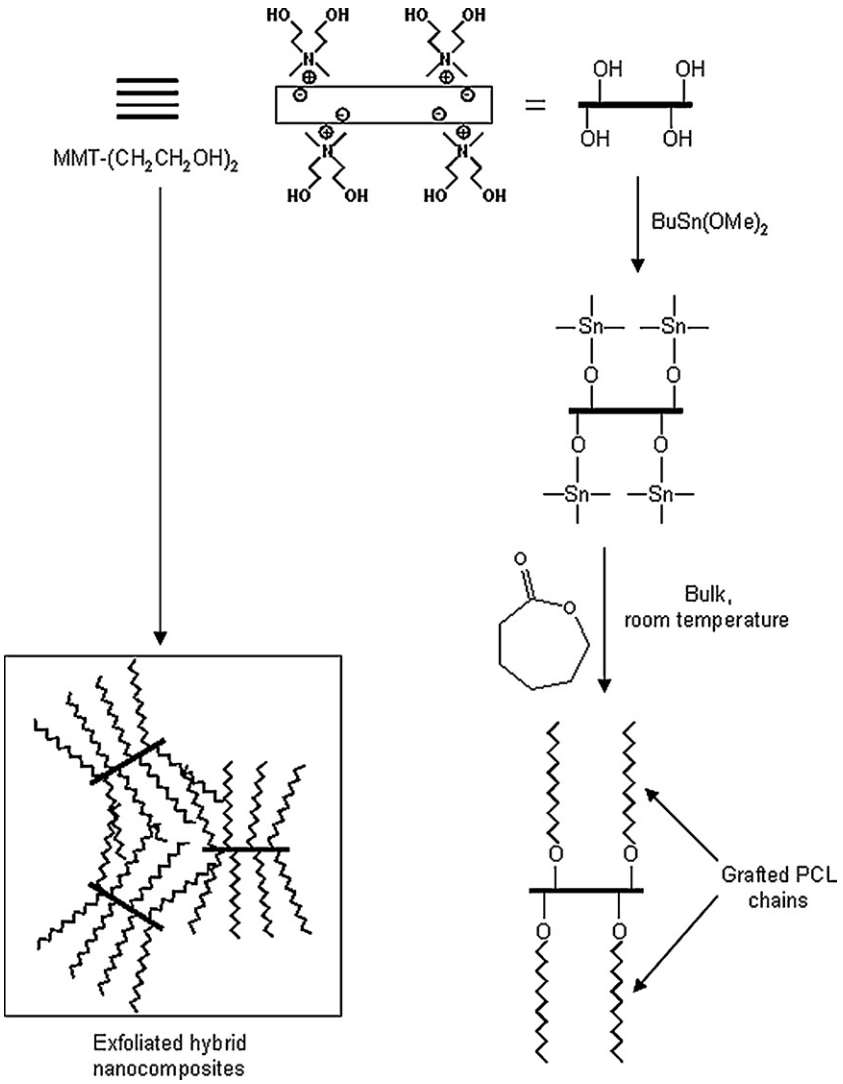

Fig. 13. Scheme of the ε-CL in-situ ring-opening polymerization from the C30B organoclay according to the "coordination-insertion" mechanism. Reproduced with permission from Lepoittevin et al. [137] copyright (2002) of the American Chemical Society.

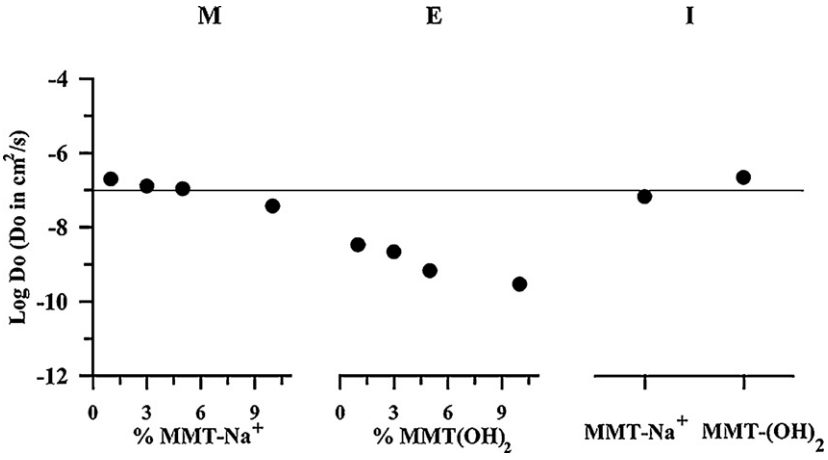

Fig. 14. log D_0 (D_0 in cm^2/s) to water vapor, as function of clay content for the PCL microcomposite (*M*), the exfoliated PCL nanocomposites (*E*) and the 3 wt% intercalated PCL nanocomposites (*I*). Reproduced with permission from Gorrasi et al. [142] copyright (2003) of Elsevier Science Ltd.

nium bearing hydroxyl groups (MMT-$N^+(Me)_2(EtOH)(C_{16})$ or MMT-$N^+(Me)(EtOH)_2$(tallow)) and then adding an initiator/activator such as tin(II) octoate ($Sn(Oct)_2$), dibutyltin-(IV) dimethoxide ($Bu_2Sn(OMe)_2$) or triethylaluminium ($AlEt_3$). The ammonium is thus activated and can yield surface grafted PCL chains. Every hydroxyl function generates a PCL chain. Consequently, the higher the hydroxyl groups content, the lower the PCL average molar masses. It is worth noting that, in the presence of tin(IV) catalysts, since they are more efficient towards ε-CL ROP, the preparation took place in milder conditions compared to $Sn(Oct)_2$ [135]. Moreover, in all cases, the nanocomposites exhibited a continuous decrease of molar masses with clay concentration. This can be explained by OH functions, which can act both as co-initiator and chain transfer agent. This in-situ polymerization process led to well-exfoliated PCL-based nanocomposites with 3 wt% of clay while with higher content (10 wt%) partially exfoliated/partially intercalated structures were observed. Further morphological observations were carried out by scanning probe microscopy (SPM), while surface analysis was examined by X-ray photoelectron spectroscopy (XPS) and Fourier transform infrared spectroscopy in the reflection absorption mode (FT-IRAS) [141]. Taking into account the structure, the thermal stability increased and the water permeability decreased (see Fig. 14) since the well-dispersed fillers with high aspect ratio acted as barriers to oxygen and volatile degradation products [135,142]. In contrast, nanocomposites filled with non-hydroxyl functional clays exhibited only intercalated structures [136,137,140].

Since ε-CL polymerization is initiated by OH groups, polymer chains lengths can be predetermined and controlled by the clay loading. Thus, the clay content is limited to a certain range of concentrations to prevent from obtaining too short PCL chain lengths. Nevertheless, this can be modulated by tuning the number of OH groups, e.g., by modifying the clay surface by a mixture of non-functional alkylammonium and monohydroxylated ammonium cations [138,139,143]. Thus, using this interesting in-situ intercalative process, the inorganic content, the quantitative surface grafting, the number of polyester chains per clay surface as well as the polymer chain length and molecular weight distribution are well controlled [139]. Viville et al. [143] also studied the morphology of PCL grafted chains on the silicate layer surface depending on the OH content. They showed that the grafting density drastically increased as the proportion of OH-substituted alkylammonium cations used to organomodify the clay increased. Since separate polymer islands were formed in the low OH systems (see Fig. 15), they assumed that a phase separation process occurred between the ammonium ions induced by the polymerization reaction. Homogeneous coverage and subsequent thickening only take place from 50% OH content. When this situation was achieved, adjacent platelets become fully independent of each other, which greatly favored exfoliation.

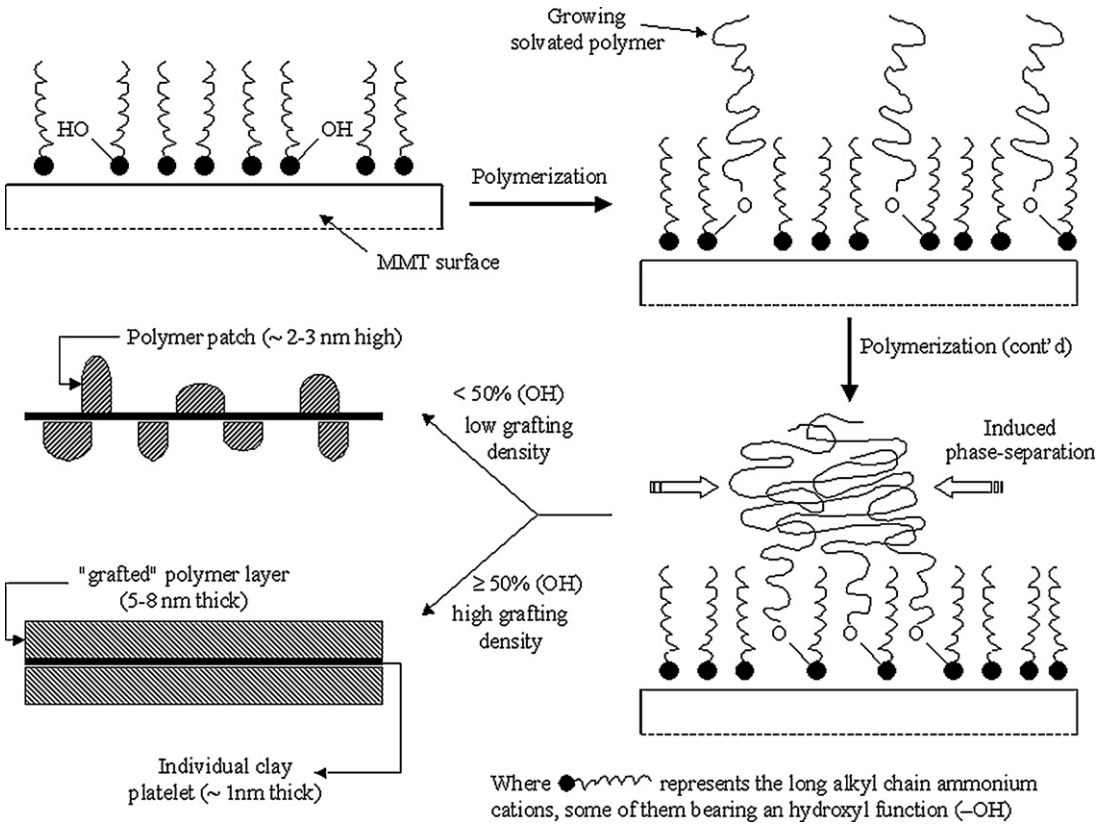

Fig. 15. Polymer surface grafting onto individual clay platelets and concomitant phase separation. Reproduced with permission from Viville et al. [143] copyright (2004) of the American Chemical Society.

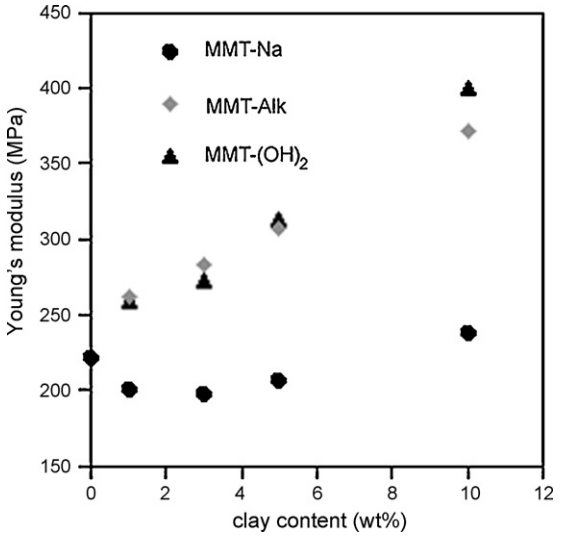

Fig. 16. Dependence of Young's modulus on the clay content for PCL modified by CNa, C25A and C30B. Reproduced with permission from Lepoittevin et al. [145] copyright (2002) of Elsevier Science Ltd.

The "coordination-insertion" mechanism, i.e., in-situ intercalation catalyzed by initiators, was compared to the thermally activated in-situ intercalation with various OMMT [140]. Messersmith and Giannelis' results [127] stating that large catalytic surface of montmorillonite can contribute to polymerization of ε-CL were confirmed. Exchanged cations bearing protic functions like NH_3^+, OH, COOH significantly favored the polymerization and lead to similar structures to those obtained by the "coordination-insertion" mechanism. Nevertheless, the PCL molecular weights remained low and the polydispersity index at high conversion reached values higher than 2, confirming that the in-situ intercalation in presence of OH groups and initiators provides better polymerization control.

Eventually, the melt intercalation route led to intercalated or intercalated/exfoliated structures when PCL was associated with OMMT bearing quaternized octadecylamine (MMT-$NH_3^+(C_{18})$), di(hydrogenated tallow) dimethyl ammonium (MMT-$N^+(Me)_2(tallow)_2$), dimethyl 2-ethylhexyl(hydrogenated tallow) (C25A), or methyl bis(2-hydroxyethyl) (hydrogenated tallow) (C30B) [135,144,145]. On the contrary, MMT-Na and MMT organomodified with ammonium bearing 12-aminododecanoic acid (MMT-$NH_3^+(C_{11}COOH)$) formed microcomposites since no change of interlayer gap was observed whereas the in-situ intercalation showed exfoliation in the case of MMT-$NH_3^+(C_{11}COOH)$ [127,135,140]. Therefore, contrary to the in-situ intercalative process, complete exfoliation was not reached by the melt intercalation route, whatever the OMMT considered (see Table 6). However, the tensile and thermal properties were improved. For instance, the modulus increased from 210 MPa for unfilled PCL to 280 MPa or 400 MPa with 3 wt% of MMT-$NH_3^+(C_{18})$, MMT-$N^+(Me)_2(tallow)_2$ or C25A, and 10 wt% of C30B, respectively, attesting for an almost two-fold increase of the PCL rigidity in the latter case (see Fig. 16) [144,145]. Chen and Evans [146] demonstrated on similar systems that the elastic modulus trends with clay volume fraction may be interpreted using well-established theory for conventional composites, namely the Hashin–Shtrikman bounds. At OMMT content higher than 5 wt%, the elongation at break dropped off due to clay aggregation [144,145].

Dynamic mechanical measurements also revealed that with 1 wt% clay, nanocomposites materials exhibited a pseudo solid-like behavior [145]. However, Kwak and Oh [147] demonstrated that PCL chains can diffuse further into the silicate gallery due to additionally subjecting the samples to heat during the analyses and finally, extended exfoliation are achieved. The 50% weight loss temperature is shifted by 60 °C towards higher temperature on the addition of 1 wt% of clay, whereas the temperature shift is only 30 °C at 10 wt%. Thus, PCL nanocomposites combine high stiffness, good ductility and improved thermal stability at low clay content (<5 wt%).

Only Di et al. [148] reached exfoliated state in the case of PCL/C30B systems prepared by direct melt intercalation with 2–5 wt% of clay. Obviously, they reported great enhancements of mechanical and thermal properties as well as a pseudo solid-like rheological behavior caused by the strong interactions between the organoclay layers and PCL, and by the good dispersion of exfoliated organoclay platelets. Moreover, the isothermal crystallization behavior [149] revealed that the well-dispersed organoclay platelets act as nucleating agents, but also affected the crystals quality by the restricted chains mobility.

Since the direct melt intercalation suffers a lack of efficiency towards clay dispersion, an elaboration route combining in-situ ε-CL polymerization and material redispersion by melt intercalation was settled. This masterbatch process [150], or equivalent [151], yielded intercalated/exfoliated structures that are rather difficult to reach by direct melt blending. This process also turned out to be a good way to compatibilize and thus to reinforce other thermoplastics like conventional polymers (SAN [131,152], PVC [150], PC [153], PP, PE, PS and ABS [154],) or biopolymers (PBS, PBAT [155]). Conversely, PCL was blended by a reactive process with thermoplastic-clay systems [156,157] to improve the properties of the final material.

A remarkable study on the nanocomposite preparation of oligo-PCL/OMMT by simply mechanical mixing was reported by Maiti [158]. Different types of clays having different aspect ratios (hectorite, mica, smectite) organomodified with various phosphonium cations were selected to investigate their influence on miscibility with oligo-PCL (o-PCL). The alkyl phosphonium cations were *n*-octyltri-*n*-butylphosphonium ($P^+(But)_3(C_8)$), *n*-dodecyltri-*n*-butylphosphonium (($P^+(But)_3(C_{12})$), *n*-hexadecyltri-*n*-butylphosphonium ($P^+(But)_3(C_{16})$) and methyltriphenylphosphonium ($P^+(Me)(\phi)_3$). Immiscible, intercalated, and exfoliated nanostructures were observed in o-PCL nanocomposites, depending on the nature of the organic modifier as well as the aspect ratio (see Table 6). Fig. 17 sums up their interpretation according to experimental results but also to thermodynamic considerations. According to Maiti, when o-PCL is immiscible with a certain organic modifier, it cannot intercalate into the

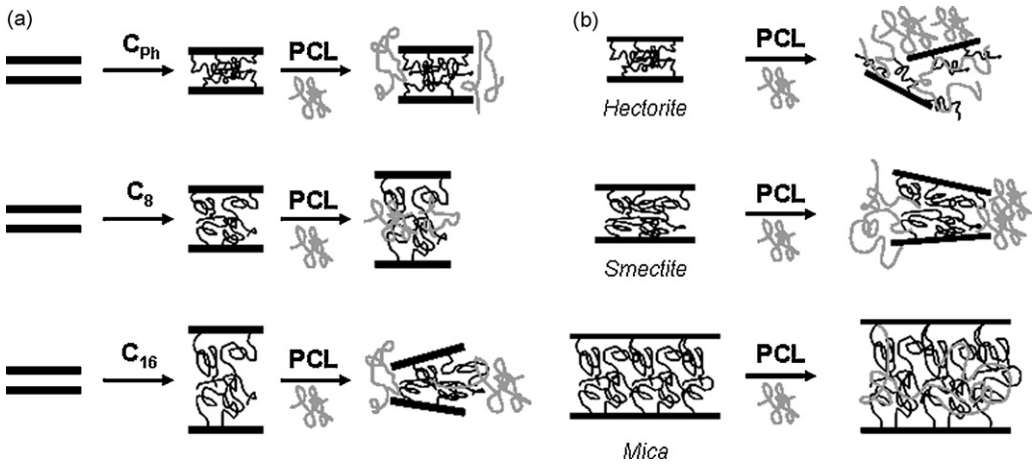

Fig. 17. Schematic representation of PCL oligomers nanocomposites depending (a) on the nature of the organomodifier and (b) on the clay aspect ratio. Reproduced with permission from Maiti [158] copyright (2003) of the American Chemical Society.

silicate gallery, while, for a short chain miscible modifier, o-PCL intercalates and, in the case of a long chain modifier, the modifier orients itself away from the silicate surface and is solubilized into the o-PCL phase, resulting in the collapse of the silicate gallery (see Fig. 17a).

Considering the effect of the aspect ratio with a given organomodifier, when the aspect ratio is low, combined with a high CEC, the organic modifier is favored to diffuse out the gallery and to interact with o-PCL leading to exfoliated structure. For higher aspect ratio, i.e., for larger lateral dimensions of the silicate layers, the organic modifier hardly access outside the gallery, and thus, the o-PCL must intercalate (see Fig. 17b).

Other works attempted to better understand the mechanism of intercalation/exfoliation process either by melt intercalation or in-situ ε-CL polymerization by molecular dynamics simulations [159–161]. Very recently, solid-state NMR has emerged as a tool to characterize clay/polymer nanocomposites in complement to data from classical methods (XRD, TEM) since it is a powerful technique for probing the molecular structure, conformation, and dynamics of species at interfaces. Therefore, solid-state NMR was used in PCL-based nanocomposites to investigate how the surfactant conformation and mobility are changed by the polymer adsorption and how the polymer motion is perturbed after intercalation in the nanocomposites [159,162,163]. Finally, Calberg et al. [159] validated this characterization method to determine the structure of PCL-based nanocomposites since they demonstrated that there was a correlation between variations in the proton relaxation times T1(H) and the quality of clay dispersion.

To conclude, PCL-based nanocomposites have been widely studied and several well-controlled routes have been settled to reach exfoliated state. To be precise, the solvent intercalation route is not one of those since no satisfactory results were obtained regarding the structure [164] (see Table 6). Excepting this, elaboration of such materials turned out to be very useful not only for PCL properties enhancement, but also for other thermoplastics ones.

4.3.2. Biodegradable aliphatic copolyester-based nano-biocomposites

4.3.2.1. Polybutylene succinate. PBS presents many interesting properties, including biodegradability, melt processability, and thermal and chemical resistance, but low gas barrier properties and softness still limit its use. Therefore, particular attention has been paid to the elaboration of PBS-based nano-biocomposites (see Table 7) to overcome these issues and to improve the material properties.

Sinha Ray et al. [165] first reported structure and properties of PBS/clay nanocomposites (PBSCN) obtained by melt intercalation. Other studies [166–168] investigated the effect of the organoclay type on the composites structures and properties. High molecular weight PBS (HMWPBS) were synthesized by a coupling reaction with a chain extender, namely the hexamethylene diisocyanate (OCN-C_6H_{12}-NCO), resulting in urethane moities (see Fig. 18) and terminal hydroxyl groups. Different OMMT were tested such as octadecylammonium and octadecyltrimethylammonium modified montmorillonite (MMT-$NH_3^+(C_{18})$ and MMT-$N^+(Me)_3(C_{18})$, respectively) and hexadecyltributylphosphonium modified saponite (SAP-$P^+(But)_3(C_{16})$). Intercalated and extended flocculated nanocomposites were obtained with the PBS/MMT-$NH_3^+(C_{18})$ systems. For MMT-$N^+(Me)_3(C_{18})$-based materials, nanocomposites showed an intercalated and flocculated structure, whereas the coexistence of the stacked intercalated and delaminated structure was observed in PBS/SAP-$P^+(But)_3(C_{16})$ nanocomposite. According to the authors, the flocculation occurred due to urethane moieties of PBS that make hydrogen bonds with the silicate hydroxyl edge groups leading to very strong interactions between matrix and silicate layers [167,168] (see Fig. 19).

These structures were confirmed, by mechanical, rheological and barrier properties. For instance, G' determined by DMA presented significant enhancements with increasing clay loading, particularly with MMT-$NH_3^+(C_{18})$ and MMT-$N^+(Me)_3(C_{18})$ since increments reached more than 200% [166]. Furthermore, since they noticed that properties of PBS/MMT-$NH_3^+(C_{18})$ and PBS/MMT-$N^+(Me)_3(C_{18})$

Table 7
Structure of the studied PBS/clay nano-biocomposites.

Process	System	Structure	Reference
Solvent intercalation	MMT-($C_5H_5N^+$)(C_{16})	Intercalated	[172]
	MMT-$N^+(Me)_3(C_{16})$	Intercalated	[172]
Melt intercalation	MMT-$NH_3^+(C_{18})$	Intercalated and flocculated	[165]
		Highly intercalated and homogeneous dispersion	[169]
	MMT-$NH_3^+(C_{18})$/HMWPBS	Intercalated and flocculated	[167]
	MMT-$NH_3^+(C_{12})$	Highly intercalated and homogeneous dispersion	[169]
	MMT-$NH_3^+(C_{11}COOH)$	Microcomposite	[169]
	MMT-$NH^+(EtOH)_2(C_{12})$	Highly intercalated and homogeneous dispersion	[169]
	MMT-$NH^+(EtOH)_2(CH_2CHOHCH_3)$	Microcomposite	[169]
	MMT-$N^+(Me)_2(C_8)$(tallow)	Intercalated	[170,171]
	GPS-g-MMT-$N^+(Me)_2(C_8)$(tallow)	Intercalated/exfoliated	[170,171]
	MMT-$N^+(Me)(EtOH)_2$(tallow)	Intercalated and flocculated	[155]
	MMT-$N^+(Me)(EtOH)_2$(tallow)/dibutyltin dilaurate	Intercalated/exfoliated	
	Or titanium butoxide	Intercalated	
	Or antimony oxide	Intercalated	
	SAP-$P^+(But)_3(C_{16})$/HMWPBS	Stacked intercalated and delaminated	[167]
Masterbatch	MMT-$NH_3^+(C_{18})$/HMWPBS + HMWPBS	Intercalated and flocculated	[166]
	MMT-$N^+(Me)_3(C_{18})$/HMWPBS + HMWPBS	Intercalated and flocculated	[166,168]
	MMT-$N^+(Me)(EtOH)_2$(tallow)-g-PCL/dibutyltin dilaurate or titanium butoxide or antimony oxide + PBS	Intercalated	[155]
	SAP-$P^+(But)_3(C_{16})$/HMWPBS + HMWPBS	Stacked intercalated and delaminated	[166]

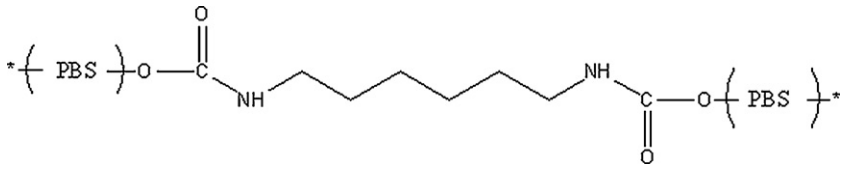

Fig. 18. HMWPBS obtained by chain extension using hexamethylene diisocyanate. Redrawn with permission from Sinha Ray et al. [167] copyright (2003) of the American Chemical Society.

suddenly increased beyond a certain clay content, they concluded to the existence of a percolation threshold value (3.3 wt% for MMT-$NH_3^+(C_{18})$) [167], and less than 3.6 wt% for MMT-$N^+(Me)_3(C_{18})$ [168]). Above this clay content, dispersed and flocculated silicate layers form a network and contribute to reinforce considerably the matrix. This structure affected the tensile properties and the rheological behavior of the PBS. Indeed, with the increasing clay content, it was shown that the tensile modulus increased while the tensile strength decreased [168]. Besides, rheologi-

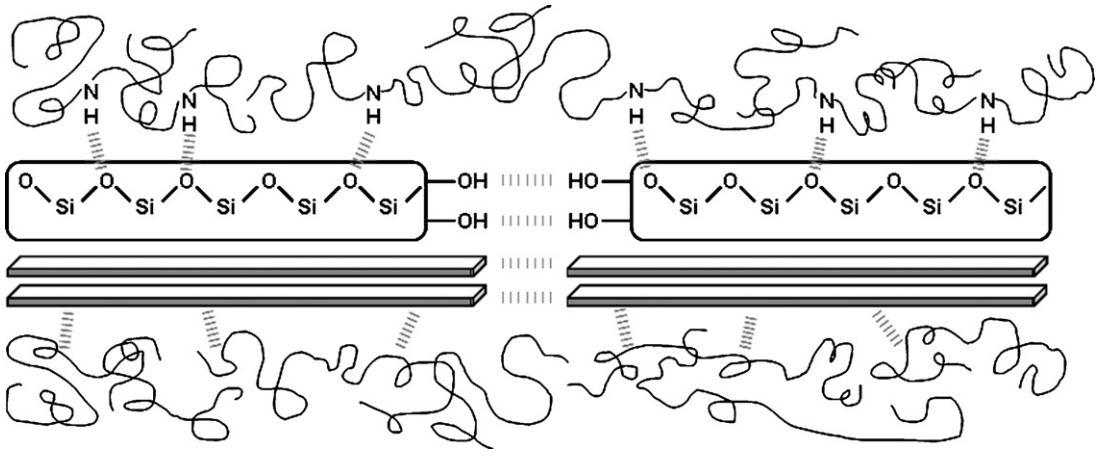

Fig. 19. Formation of hydrogen bonds between PBS and clay, leading to flocculation of the dispersed silicate layers. Reproduced with permission from Sinha Ray et al. [167] copyright (2003) of the American Chemical Society.

cal measurements revealed pseudo solid-like behavior of PBSCNs at high clay content, suggesting a prevented relaxation due to the high geometric constraints or physical jamming of the stacked silicate layers. This PBSCN structure was also confirmed by the lower slope values and the higher absolute values of the dynamic moduli [167]. Barrier properties were also consistent with flocculated and percolated structures since the O_2 permeability decreased of 52% with 3.6 wt% of MMT-$NH_3^+(C_{18})$ [166], i.e., above the percolation threshold. Eventually, on the basis of the biodegradation tests realized in compost and SEC data, authors concluded that the PBS fragmentation was significantly improved generating higher surface area for further micro-organisms attack [167].

Someya et al. [169] tested different OMMT to determine the effect of variations in hydrophobicity and polar/steric interactions. Five OMMT organomodified with primary amines (dodecylamine-MMT-$NH_3^+(C_{12})$-, octadecylamine-MMT-$NH_3^+(C_{18})$-, 12-aminolauric acid-MMT-$NH_3^+(C_{11}$COOH)) or tertiary amines (*N*-lauryldiethanolamine-MMT-$NH^+(EtOH)_2(C_{12})$-, and 1-[*N*,*N*-bis(2-hydroxyethyl)amino]-2-propanol-MMT-$NH^+(EtOH)_2(CH_2CHOHCH_3)$) were prepared and added to PBS by melt intercalation at contents from 1 to 10 wt%, and then the samples were injection molded. Highly intercalated structures and homogeneous clay dispersion were observed with MMT-$NH_3^+(C_{12})$, MMT-$NH_3^+(C_{18})$, and MMT-$NH^+(EtOH)_2(C_{12})$. On the contrary, some clusters or agglomerated particles were observed with MMT-$NH_3^+(C_{11}$COOH), MMT-$NH^+(EtOH)_2(CH_2CHOHCH_3)$, and unmodified MMT. The authors showed that the d-spacing enlargement determined by XRD was well correlated with the clay dispersion improvement and with the increase of tensile and flexural moduli and the decrease of tensile strength. Dynamic viscoelastic measurements were also consistent with structural results since PBS/MMT-$NH^+(EtOH)_2(C_{12})$ nanocomposite had higher storage modulus and glass-transition temperature. This indicated that intercalation of PBS within the OMMT layers affected the molecular motion.

Another group achieved to improve PBS properties using compatibilization approach. Chen et al. [170] proposed to graft epoxy groups onto C25A with (glycidoxypropyl)trimethoxy silane (GPS) leading to twice-functionalized organoclay (TFC, i.e., GPS-g-C25A), as already done for PLA [102]. Tethering PBS molecules to the epoxy groups on the surface of TFC was attempted through melt compounding. Higher exfoliation degrees and better properties were reached in PBS/TFC nanocomposites compared to those of PBS/C25A due to the increased PBS–TFC interfacial interactions. XRD results showed that *d*-spacing values were comparable when 10 wt% of C25A or TFC were added, but the difference of peak intensity attested that partial disruption of parallel stacking of TFC had occurred. The intercalation/exfoliation coexistence in the PBS/TFC systems has also been demonstrated by TEM images, whereas intercalated clay tactoids have been observed with C25A. The mechanical properties are increased up to 10 wt% of filler. Dynamic mechanical analyses also showed that E' was higher than that for neat PBS and increases with the clay content. Furthermore, a weak shoulder appearing at $\sim$50 °C in the tan δ profile was attributed to the relaxation of PBS segments confined within the clay layers, in agreement with the structure deduced from morphological characterizations. Eventually, the study of the non-isothermal crystallization behavior showed out that well-dispersed TFC layers enhanced the nucleation and crystallization rate of the PBS matrix [171].

C30B was also used for the preparation of 3 wt% filled PBS-based nanocomposites by melt intercalation [155]. Since the *d*-spacing increased, intercalated structure was obtained resulting in PBS rigidity improvement (+25% Young's modulus). Furthermore, authors also tested metal-based catalysts (dibutyltin dilaurate $Sn(Bu)_2(Lau)_2$, titanium(IV) butoxide $Ti(OBu)_4$ and antimony(III) oxide Sb_2O_3) to promote transesterification between the ester moiety of the PBS and the organomodifier OH groups to graft PBS chains onto the organoclay surface. $Sn(Bu)_2(Lau)_2$ appeared to be the most appropriate catalyst since XRD and TEM clearly showed higher levels of clay exfoliation. Extraction process followed by TGA showed that grafting reaction had occurred. Consequently, material stiffness improved considerably by a Young's modulus increase of +60% compared to neat PBS.

Shih et al. [172] investigated different organoclays functionalized by ammonium salts such as cetylpyridinium chloride ($(C_5H_5N^+)(C_{16})$) and cetyltrimethylammonium bromide ($N^+(Me)_3(C_{16})$), which were mixed with PBS by solvent intercalation at 1, 3 and 5 wt%. The enhancement of E' and E'' showed that the stiffness and toughness of PBS were simultaneously improved (see Fig. 20). Weak shoulders on tan δ peaks at 5 wt% of clay were observed corresponding to the relaxation of PBS segments confined within the clay platelets, suggesting an intercalated structure and inhomogeneous dispersion due to clay aggregation, as mentioned by Chen et al. [170]. However, PBS/MMT-$N^+(Me)_3(C_{16})$ nanocomposites exhibited higher storage and loss moduli than PBS/MMT-$(C_5H_5N^+)(C_{16})$ systems. Thus, aliphatic chain in $N^+(Me)_3(C_{16})$, compared to the aromatic group in cetylpyridinium, may interact more favorably with the aliphatic PBS because of their similar structures. Morphological characterizations were consistent with mechanical properties namely intercalated structures were obtained and better extent of *d*-spacing was observed with MMT-$N^+(Me)_3(C_{16})$. Furthermore, TEM confirmed the coexistence of intercalated and exfoliated structures with 3 wt% of MMT-$N^+(Me)_3(C_{16})$ nanocomposite, whereas aggregation was obtained with 5 wt% OMMT.

4.3.2.2. Polybutylene succinate-co-adipate. Sinha Ray et al. [173–176] also reported PBSA-based nanocomposites studies. First, they have investigated various types of organoclays from Southern Clay Products (C15A, C93A and C30B) which present different polarity [174] (see Table 8). XRD and TEM have shown that the polymer–clay compatibility plays a key role in attaining high *d*-spacing and high quality of dispersion. Finally, C30B appeared the most suitable nanofiller for PBSA-based nanocomposites prepared by melt intercalation. Highly disordered and exfoliated platelets coexist with a few stacked intercalated layers due to interactions between C=O groups (PBSA backbone) and OH functions (C30B). Nevertheless, the dispersion quality

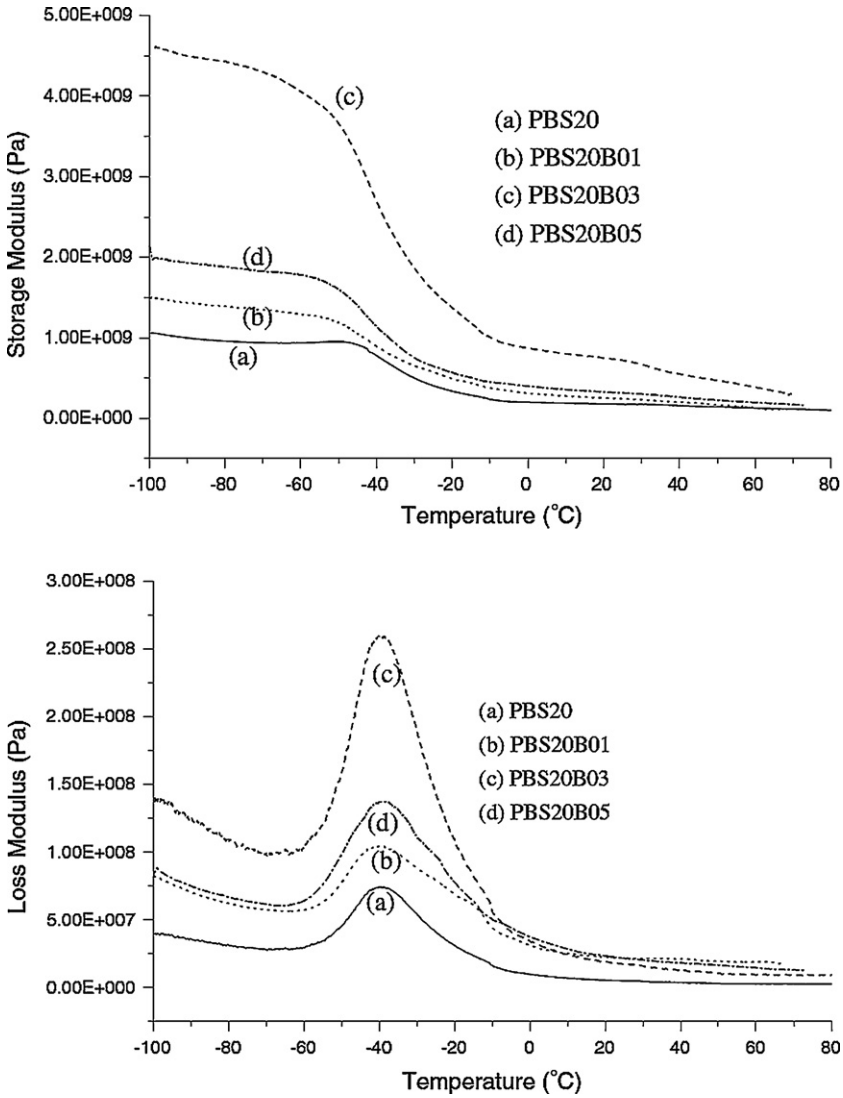

Fig. 20. Temperature dependence of the storage and loss moduli for neat PBS (a) and PBS composites (b–d) with respectively 1, 3 and 5 wt% of MMT-($C_5H_5N^+$)(C_{16}). Reproduced with permission from Shih et al. [172] copyright (2007) of Springer Science.

Table 8
Structure of the studied PBSA/clay nano-biocomposites.

Process	System	Structure	Reference
Solvent intercalation	MMT-$N^+(Me)_2(C_8)$(tallow)/chloroform	Intercalated	[177,178]
	MMT-$N^+(Me)_2(C_8)$(tallow)/poly(epichlorohydrin)/methylene chloride	Intercalated	[180,181]
Melt intercalation	MMT-$N^+(Me)(EtOH)_2$(tallow)	Exfoliated (high clay content)	[64]
		Intercalated (low clay content)	[173,174]
		Intercalated/exfoliated	
	MMT-$N^+(Me)_2(C_8)$(tallow)	Intercalated	[179]
	MMT-$NH^+(Me)$(tallow)$_2$	Intercalated	[174]
	MMT-$N^+(Me)_2(C_8)$(tallow)	Intercalated	[174]
	GPS-g-MMT-$N^+(Me)_2(C_8)$(tallow)	Intercalated	[182]
	MPS-g-MMT-$N^+(Me)_2(C_8)$(tallow)		
	SFM-$N^+(Me)(EtOH)_2$(coco alkyl)	Intercalated/exfoliated	[176,183]

was lowered with increasing clay content [173]. Consequently, thermal and mechanical properties were affected by the clay induced structure according to the nature and content of organoclay. First, although the PBSA crystal structure was not altered by the incorporation of clay, the crystallinity systematically decreased with the increasing dispersion degree of silicate layers into PBSA matrix. In the case of strong polymer–clay interactions, the mobility and flexibility of the polymer chains are hindered, limiting their ability to fold and participate to the crystallization growth front. A significant increase in E' was observed due to the intercalation of chains within the silicate layers and this increase was more important with higher C30B content [173]. Furthermore, it was also shown a substantial increase for E'' suggesting the presence of strong internal friction between homogeneously dispersed intercalated silicate particles. Tensile properties were also examined: the tensile modulus and elongation at break increased in presence of organoclay, but the improvement was strongly dependent on the degree of dispersion and on the C30B content. These improvements were only due to the structure formation since crystallinity decrease on addition of clays. The rheological properties also pointed out a gradual change of behavior from liquid-like to solid-like with the increasing polymer-OMMT affinity. These results were mainly attributed to the extent of dispersion and distribution of the clay lamellae that form, beyond a threshold concentration (3 wt% in the case of C30B), three dimensional percolating networks rendering the system highly elastic. Eventually, better thermal stability was obtained for PBSA/C30B, but this enhancement was limited to low clay content since a decrease was observed above 9 wt%, probably due to the excess of organic modifier containing OH groups on the clay surface, which undergoes Hofmann degradation at around 200 °C.

Lee et al. [64] also tested C30B dispersion in Skygreen® at various clay contents ranging from 1 to 30 wt% by melt intercalation. The highest content values are unusual for nanocomposites since high content promotes aggregation. Nevertheless, in this case, exfoliated states were achieved above 15 wt% whereas intercalation was obtained with lower clay contents. The authors attributed this phenomenon to the combination of high shear rate reached during melt intercalation and the polymer-OMMT affinity. As seen before [96,97,121], strong interactions or miscibility exist between the polymer and the C30B, due to strong hydrogen bonding between the carboxyl group from the biodegradable polyester and the OH group from C30B. These results were confirmed by TEM since the nanocomposites showed ordered intercalated structures with expanded layer gap and good dispersion at 10 wt%. Tensile properties enhancements were consistent with the structural results. The nanocomposite biodegradability decreased with increasing organoclay amount. This behavior was explained by the difficulty for micro-organisms to reach the bulk matrix due to the presence of dispersed clay layers with large aspect ratio that make the diffusion path more tortuous.

C25A was also tested as a nanofiller to improve Skygreen® properties [177–180]. Regardless of the elaboration route, solvent [177,178] or melt intercalation [179], or the organoclay content studied (<15 wt%), intercalated structures were observed. Even for Skygreen® blended with polyepichlorohydrin (PECH), no larger d-spacing was obtained [180,181], although the interlayer gap of PECH/OMMT nanocomposites can attain high values (>55 Å). Moreover, TEM observations but also the decrease and the broadening of d_{001} peak intensity with the decreasing clay content supposed that structures were much more inhomogeneous at low clay content showing exfoliated platelets at 3 wt% of C25A [179]. Rheological measurements showed that shear–thinning behavior and solid-like properties at low frequency region were enhanced by the addition of organoclay. These characterization techniques also led to definition of a critical volume fraction. Beyond that threshold, the tactoids and individual layers are prevented from relaxing completely when subjected to shear, due to physical jamming or percolation, leading to the solid-like behavior observed in both intercalated and exfoliated nanocomposites. Creep and recovery tests were found consistent with these conclusions. Although the tensile modulus dramatically increases with the clay content, the elongation at break decreases and the onset temperature of thermal decomposition drop beyond a certain clay loading [178]. The collapse of mechanical and thermal properties is attributed to the OMMT aggregation. However, regarding the thermal stability in the presence of C25A, with or without PECH, the decomposition phenomenon in terms of onset temperature and degradation rate is not fully understood. In this case, the decomposition rate increased with the increasing clay content, while the onset degradation temperature was improved [178]. Authors then supposed that, in a first step, the clay acts as a heat barrier and leads to the char formation after thermal decomposition. However, in a second step, the tactoids domain could hold accumulated heat, which could be a source, in conjunction with the heat flow supplied by the external heat source, to accelerate the decomposition process.

C25A was further modified by Chen and Yoon [182], based on the protocol established for PLLA-based [102] and PBS-based nanocomposites [170]. The C25A was functionalized by grafting epoxy group at the surface using silane coupling agent. In this case, they tested (glycidyloxypropyl)trimethoxy silane (GPS) and (methacryloyloxypropyl)trimethoxy silane (MPS) as coupling agents. According to the authors, the silane compounds are located mainly on the edge of the silicate layers where the concentration of the silanol groups is higher than on the plain surface. The preparation of the resulting twice-functionalized clay (TFC, i.e., GPS-g-C25A or MPS-g-C25A) is shown in Figs. 6 and 7. From XRD and TEM, it was concluded that both the reaction between the PBSA end-groups and the GPS-g-C25A epoxy groups, and the polar interaction between the ester groups in MPS-g-C25A and PBSA, should have enhanced the compatibility. A larger increase of d-spacing and better clay layers dispersion were observed with 2 wt% of GPS-g-C25A or MPS-g-C25A, compared to same C25A loading. The macroscopic properties were improved too. The storage modulus of PBSA/TFC was much higher than that of PBSA/C25A, especially in the low-frequency region, and non-terminal behavior was observed

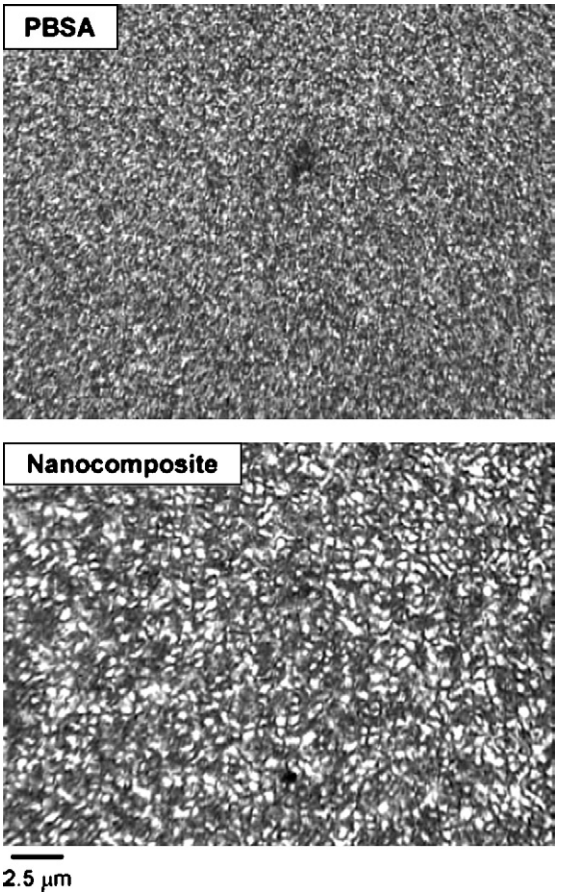

Fig. 21. Polarized optical microscopy images of PBSA and its nanocomposite with 6 wt% of SFM-N_+(Me)$(EtOH)_2$(coco alkyl) recorded at 70 °C during non-isothermal crystallization from their melts (150 °C) at a cooling rate of 10 °C min^{-1}. Reproduced with permission from Sinha Ray and Bousmina [183] copyright (2006) of Wiley-VCH.

at the terminal zone as a result of the enhanced PBSA–TFC interactions. Tensile modulus and strength at break were greatly improved with GPS-g-C25A and MPS-g-C25A due to the increased interfacial interaction.

A study of PBSA/synthetic fluorinated mica nanocomposites was carried out by Sinha Ray et al. [176,183]. Organomodified SFM (OSFM, Somasif from CO-OP Chemicals Ltd.) was melt mixed with Bionolle®. The resulting nanocomposites showed that some intercalated stacked and disordered and/or exfoliated silicate layers coexist. The thermo-mechanical properties were improved over the temperature range investigated, and particularly above the T_g since E' increased by more than 100% compared to neat PBSA. Considering the crystallization behavior [183], the non-isothermal crystallization kinetics of the nanocomposite and its higher activation energy calculated from model were in agreement with prior results [173]. Namely, the incorporation of OSFM slows the nucleation mechanism and PBSA crystal growth as a result of the full dispersion of silicate layers into the matrix, which act as obstacles (see Fig. 21). The homogeneous dispersion was shown to increase the cold crystallization temperature of the nanocomposite. Three prominent melting endotherms of PBSA resulting from the melting–recrystallization process were shifted towards lower temperature and decreased in intensity due to the clay dispersion that restricted the motions of polymer chains. Besides, the thermal stability of PBSA was moderately increased in the presence of OSFM under both nitrogen and air atmospheres overall thermal degradation temperature range. In the early stage of the decomposition, although the surfactant, and thus the nanocomposite, seemed to be more prone to degrade in thermo-oxidative conditions than pyrolytic conditions, the main degradation temperature and char formation were increased in air compared to nitrogen. According to authors, the different types of char formation mechanisms under oxidative environment actually slow the oxygen diffusion, thus hindering the oxidation procedure under thermo-oxidative conditions. Consequently, the flame retardance property of the nanocomposite was improved. To conclude, the activation energy of the nanocomposite thermal degradation calculated from the Kissinger model was slightly higher than that of neat PBSA, in agreement with previous results [174,178]. Classical and original processes were investigated as means to reach an exfoliated state and improved aliphatic copolyester-based nano-biocomposites properties, with more-or-less success (see Table 8). Furthermore, whatever the systems considered, the properties were well correlated to the materials structures.

4.3.3. Aromatic copolyester-based nano-biocomposites

PBAT is flexible and has a higher elongation at break than most biodegradable polyesters, such as PLA and PBS, and therefore is more suitable for food packaging and agricultural films. Only few articles report studies of PBAT/clay nano-biocomposites (see Table 9).

Recently, Someya et al. [184] have prepared OMMT which have been proved to be the more efficient with PBS [169], i.e., MMT-$NH_3^+(C_{12})$, MMT-$NH_3^+(C_{18})$, MMT-$NH^+(EtOH)_2(C_{12})$. They investigated the morphology and the properties of PBAT/clay nanocomposites prepared by melt intercalation containing 3–10 wt% OMMT. Intercalation occurred in the case of MMT-$NH_3^+(C_{12})$ and MMT-$NH^+(EtOH)_2(C_{12})$ and exfoliation, in addition to some intercalation, occurred with MMT-$NH_3^+(C_{18})$, which was also more finely dispersed in the matrix. Authors demonstrated that the mechanical properties were related to the structure as well as the crystallinity of the nanocomposites, leading globally to higher properties for PBAT/MMT-$NH_3^+(C_{18})$. Furthermore, they showed that the clay reinforcing effect is really effective above T_g, because of restricted polymer chains motions. Biodegradability was evaluated by the aerobic tests both in the soil and the aqueous medium containing activated sludge [185]. Compared to neat PBAT, the microcomposite based on unmodified montmorillonite exhibited a higher weight loss than PBAT/MMT-$NH_3^+(C_{18})$ nanocomposites.

Chivrac et al. [186,187] have expanded this work, testing various organoclays such as C20A, D43B and N804. The results relating to the structure and properties were compared to neat PBAT and the PBAT/MMT-Na, i.e., with non-modified montmorillonite. They also compared elaboration processes, i.e., solvent or melt intercalation. This study revealed that higher intercalation degrees were

Table 9
Structure of the studied PBAT/clay nano-biocomposites.

Process	System	Structure	Reference
Solvent intercalation	MMT-$N^+(Me)_2(tallow)_2$/chloroform MMT-$N^+(Me)_2(CH_2$-$\phi)$(tallow)/chloroform	Intercalated	[186]
Melt intercalation	MMT-$NH_3^+(C_{12})$	Intercalated	[184]
	MMT-$NH_3^+(C_{18})$	Intercalated/exfoliated	[184]
	MMT-$NH^+(EtOH)_2(C_{12})$	Intercalated	[184]
	MMT-$N^+(Me)_2(tallow)_2$	Intercalated	[186]
	MMT-$N^+(Me)_2(CH_2$-$\phi)$(tallow)	Intercalated	[186]
	MMT-$N^+(Me)(EtOH)_2$(tallow)	Intercalated	[155]
Masterbatch	MMT-$N^+(Me)(EtOH)_2$(tallow)-g-PCL + PBAT	Intercalated	[155]

obtained by solvent intercalation, C20A and D43B presenting better affinity with PBAT. No impact of the clay has been noticed on the T_g and T_m, whereas the crystallinity was affected by increasing clay content. Thus, they investigated the influence of the clay on the PBAT crystallization [187]. Kinetics models were applied and it was concluded that addition of a small amount of MMT enhances the PBAT nucleation mechanism, but also hinders crystallite growth. These two antagonist phenomena lead to different crystallization behavior depending on the clay dispersion. Furthermore, tensile tests have shown that the stiffness increases continuously with clay content. This was attributed to the existence of strong interactions between PBAT and nanofillers, particularly with C20A, since the crystallinity decreases with increasing clay content. Nevertheless, decreases of the strain at yield and at break have been observed due to more aggregated structures at higher clay contents (see Fig. 22). The onset degradation temperatures have been examined by TGA. The highest improvements were observed for nano-biocomposites filled with 3 wt% of MMT-Na. However, a decrease of the onset degradation temperatures is observed for higher clay contents, both with melt and solvent intercalations. This phenomenon is similar to the one described before by Lim et al. [178], i.e., clays act as heat barrier and lead to char formation after thermal decomposition, but unfortunately, tactoids can accumulate heat which could be used to accelerate the decomposition reaction.

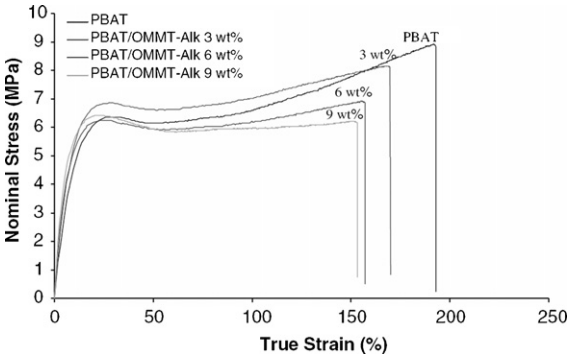

Fig. 22. Typical tensile curves obtained for neat PBAT and PBAT nanocomposites with 3, 6 and 9 wt% of C20A. Reproduced with permission from Chivrac et al. [186] copyright (2006) of Springer Science.

To conclude, a large range of OMMT has been tested, leading to different PBAT-based nanocomposites structures. These studies thus highlighted the relationship between the materials structures and their properties.

4.3.4. Polyesteramide-based nano-biocomposites

Because, the polyesteramide presents high water permeability (see Table 1), it appears necessary to improve this property, particularly if such materials are aimed at packaging applications.

Krook et al. [188,189] studied the barrier and mechanical properties of biodegradable melt-mixed polyesteramide/octadecylamine-treated montmorillonite (MMT-$NH_3^+(C_{18})$) containing 5 or 13 wt% of clay processed in different conditions (temperature, extruder screw speed). An increase of *d*-spacing was observed, suggesting that intercalated structures were reached upon extrusion. A decrease in XRD peak intensity with increasing screw speed was observed, which implied that higher shear rates promoted delamination. TEM observations indicated that clay stacks were delaminated into smaller aggregates, containing generally one to three clay sheets. They also showed the presence of shear-induced voids almost exclusively located between the clay layers, which was confirmed by density measurements. These voids limited the improvement in barrier properties. The oxygen and water vapor transmission rates decreased with increasing clay content. According to the authors, the presence of voids prevents gas diffusion through the film. The low barrier properties improvement was due to the non-uniformly dispersed clay particles. However, the large improvement in stiffness and strength with filler content indicated that the mechanical properties were unaffected by the voids.

Authors have also highlighted that the void content was reduced by compression molding after extrusion. This treatment led to higher crystallinity. This behavior induces lower gas transmission rates and higher mechanical properties (stiffness, yield point at higher stress levels).

These results were completed with a series of injection-molded samples [189]. XRD and TEM showed that these samples contained clay stacks. However, TEM also revealed that clay layers were largely delaminated and oriented "unidirectionally" over several microns. The transport and mechanical properties were greatly improved. This was attributed to a combined effect of a lower void content, higher crystallinity and greater degree of orientation.

To conclude, since packaging applications are considered for these materials, characterizations were focused on mechanical and barrier properties. The elaboration process was optimized to ensure good dispersion of clay and to avoid defects. Further properties were tested like optical transparency, weld strength, hot tack and transport properties [188].

5. Conclusion

This review presents the state of the art in biopolyester/clay nano-biocomposites. It has been clearly demonstrated that different parameters such as elaboration route, polymer/clay affinity and clay content can affect the structure and the nano-biocomposites properties. These latter can consequently be tuned as desired by controlling the parameters previously mentioned. It has to be noted that the higher reinforcing effect is generally limited to small clay amounts (<5 wt%) and is reached for exfoliated states, which are not so trivial to obtain. Indeed, although the more convenient clays to obtain delaminated platelets into biopolyesters appear to be those matching the matrix polarity, i.e., clay with organomodifier bearing at least one hydroxyl group, structure also depends on the elaboration process. Considering PLA and PCL matrices, nano-biocomposites with highly exfoliated clays can be obtained thanks to a well controlled in-situ polymerization process, whereas the melt and/or solvent intercalation methods lead to more aggregated structures. Thus, for some biopolyester matrices like PHA, aliphatic or aromatic polyesters, exfoliated states were not reported or clearly demonstrated. Eventually, temperature sensitivity of some biopolyesters can also prevent good clay delamination and properties enhancement.

In the case of good delamination and dispersion of clays, the mechanical reinforcement, thermal stability, biodegradability and barrier properties were generally improved. Rheological measurements also revealed that nano-biocomposites could present a more-or-less pronounced pseudo solid-like behavior indicating restricted motions of the biopolymer chains.

Finally, nano-biocomposites present concurrent improvement in various material properties at very low filler content, using conventional plastic processing in the elaboration. Nano-biocomposites usefulness is no longer in question, and more and more reports are focussed on application aspects in the environment, packaging, agriculture devices, biomedical fields, etc. Moreover, since industry is concerned with sustainable developments, the production cost of biopolymers goes on decreasing, which will allow strong developments of biopolymers-based materials, such as the nano-biocomposites. Therefore, these materials will be technically and financially competitive towards synthetic polymer-based nanocomposites, opening a new dimension for the plastic industry.

Future research will address some actual issues such as the difficulty to exfoliate the clay with some biopolyester matrixes (e.g., PHA). Further work should furnish valuable insight into new methods of nano-biocomposites designed to establish new approaches to tailor novel nano-architectures.

References

[1] Kaplan DL, Mayer JM, Ball D, McCassie J, Allen AL, Stenhouse P. Fundamentals of biodegradable polymers. In: Ching C, Kaplan DL, Thomas EL, editors. Biodegradable polymers and packaging. Lancaster: Technomic Pub. Co.; 1993. p. 1–42.

[2] Kaplan DL. Biopolymers from renewable resources. Berlin: Springer Verlag; 1998.

[3] Chandra R, Rustgi R. Biodegradable polymers. Prog Polym Sci 1998;23:1273–335.

[4] Steinbuchel A. Biopolymers, general aspects and special applications. Weinheim, Germany: Wiley-VCH; 2003.

[5] Averous L, Boquillon N. Biocomposites based on plasticized starch: thermal and mechanical behaviors. Carbohydr Polym 2004;56:111–22.

[6] Averous L. Polylactic acid: synthesis, properties and applications. In: Belgacem N, Gandini A, editors. Monomers, oligomers, polymers and composites from renewable resources. Oxford: Elsevier Limited Publication; 2008. p. 433–50.

[7] Garlotta D. A literature review of poly(lactic acid). J Polym Environ 2001;9:63–84.

[8] Wee Y-J, Kim J-N, Ryu H-W. Biotechnological production of lactic acid and its recent applications. Food Technol Biotech 2006;44:163–72.

[9] Moon SI, Lee CW, Miyamoto M, Kimura Y. Melt polycondensation of L-lactic acid with Sn(II) catalysts activated by various proton acids: a direct manufacturing route to high molecular weight poly(L-lactic acid). J Polym Sci Polym Chem 2000;38:1673–9.

[10] Moon S-I, Lee C-W, Taniguchi I, Miyamoto M, Kimura Y. Melt/solid polycondensation of L-lactic acid: an alternative route to poly(L-lactic acid) with high molecular weight. Polymer 2001;42:5059–62.

[11] Okada M. Chemical syntheses of biodegradable polymers. Prog Polym Sci 2002;27:87–133.

[12] Albertsson A-C, Varma IK. Aliphatic polyesters: synthesis, properties and applications. Adv Polym Sci 2002;157:1–40.

[13] Vert M, Schwarch G, Coudane J. Present and future of PLA polymers. J Macromol Sci A 1995;32:787–96.

[14] Sinclair RG. The case for polylactic acid as a commodity packaging plastic. J Macromol Sci A 1996;33:585–97.

[15] Lunt J. Large-scale production, properties and commercial applications of polylactic acid polymers. Polym Degrad Stabil 1998;59:145–52.

[16] Auras R, Harte B, Selke S. An overview of polylactides as packaging materials. Macromol Biosci 2004;4:835–64.

[17] Steinbuchel A, Doi Y. Polyesters III—applications and commercial products. Weinheim, Germany: Wiley-VCH; 2002.

[18] Bigg DM. Effect of copolymer ratio on the crystallinity and properties of polylactic acid copolymers. In: Proceedings of the 54th annual technical conference of the society of plastics engineers, vol. 2. Boca Raton (FL), USA: Published by CRC Press; 1996. p. 2028–39.

[19] Perego G, Cella GD, Bastioli C. Effect of molecular weight and crystallinity on poly(lactic acid) mechanical properties. J Appl Polym Sci 1996;59:37–43.

[20] Cartier L, Okihara T, Ikada Y, Tsuji H, Puiggali J, Lotz B. Epitaxial crystallization and crystalline polymorphism of polylactides. Polymer 2000;41:8909–19.

[21] Martin O, Averous L. Poly(lactic acid): plasticization and properties of biodegradable multiphase systems. Polymer 2001;42:6209–19.

[22] Labrecque LV, Kumar RA, Dave V, Gross RA, McCarthy SP. Citrate esters as plasticizers for poly(lactic acid). J Appl Polym Sci 1997;66:1507–13.

[23] Jacobsen S, Fritz HG. Plasticizing polylactide—the effect of different plasticizers on the mechanical properties. Polym Eng Sci 1999;39:1303–10.

[24] Kranz H, Ubrich N, Maincent P, Bodmeier R. Physicomechanical properties of biodegradable poly(D,L-lactide) and poly(D,L-lactide-co-glycolide) films in the dry and wet states. J Pharm Sci US 2000;89:1558–66.

[25] Ljungberg N, Andersson T, Wesslen B. Film extrusion and film weldability of poly(lactic acid) plasticized with triacetine and tributyl citrate. J Appl Polym Sci 2003;88:3239–47.

[26] Van Tuil R, Fowler P, Lawther M, Weber CJ. Properties of biobased packaging materials. In: Biobased packaging materials for the food industry—status and perspectives. Frederiksberg, Denmark: KVL; 2000. p. 8–33.

[27] Lehermeier HJ, Dorgan JR, Way JD. Gas permeation properties of poly(lactic acid). J Membr Sci 2001;190:243–51.

[28] McCarthy SP, Ranganthan A, Ma W. Advances in properties and biodegradabilility of co-continuous, immiscible, biodegradable, polymer blends. Macromol Symp 1999;144:63–72.
[29] Bastioli C. Biodegradable materials—present situation and future perspectives. Macromol Symp 1998;135:193–204.
[30] Tuominen J, Kylma J, Kapanen A, Venelampi O, Itävaara M, Seppälä J. Biodegradation of lactic acid based polymers under controlled composting conditions and evaluation of the ecotoxicological impact. Biomacromolecules 2002;3:445–55.
[31] De Koning GJM. Prospects of bacterial poly[(*R*)-3-hydroxyalkanoates]. PhD Thesis. Eindhoven: Eindhoven University of Technology; 1993.
[32] Madison LL, Huisman GW. Metabolic engineering of poly(3-hydroxyalkanoates): from DNA to plastic. Microbiol Mol Biol Rev 1999;63:21–53.
[33] Doi Y. Microbial polyesters. New York: John Wiley & Sons, Inc.; 1990.
[34] Zinn M, Witholt B, Egli T. Occurrence, synthesis and medical application of bacterial polyhydroxyalkanoate. Adv Drug Deliv Rev 2001;53:5–21.
[35] Valentin HE, Broyles DL, Casagrande LA, Colburn SM, Creely WL, DeLaquil PA, et al. PHA production, from bacteria to plants. Int J Biol Macromol 1999;25:303–6.
[36] Poirier Y. Polyhydroxyalkanoate synthesis in plants as a tool for biotechnology and basic studies of lipid metabolism. Prog Lipid Res 2002;41:131–55.
[37] Hori Y, Suzuki M, Yamaguchi A, Nishishita T. Ring-opening polymerization of optically active β-butyrolactone using distannoxane catalysts: synthesis of high-molecular-weight poly(3-hydroxybutyrate). Macromolecules 1993;26:5533–4.
[38] Hori Y, Takahashi Y, Yamaguchi A, Nishishita T. Ring-opening copolymerization of optically active β-butyrolactone with several lactones catalyzed by distannoxane complexes: synthesis of new biodegradable polyesters. Macromolecules 1993;26:4388–90.
[39] Hori Y, Hagiwara T. Ring-opening polymerisation of β-butyrolactone catalysed by distannoxane complexes: study of the mechanism. Int J Biol Macromol 1996;25:235–47.
[40] Kobayashi T, Yamaguchi A, Hagiwara T, Hori Y. Synthesis of poly(3-hydroxyalkanoate)s by ring-opening copolymerization of (*R*)-β-butyrolactone with other four-membered lactones using a distannoxane complex as a catalyst. Polymer 1995;36:4707–10.
[41] Nobes GAR, Kazlauskas RJ, Marchessault RH. Lipase-catalyzed ring-opening polymerization of lactones: a novel route to poly(hydroxyalkanoate)s. Macromolecules 1996;29:4829–33.
[42] Juzwa M, Jedlinski Z. Novel synthesis of poly(3-hydroxybutyrate). Macromolecules 2006;39:4627–30.
[43] Asrar J, Mitsky TA, Shah DT. Polyhydroxyalkanoates of narrow molecular weight distribution prepared in transgenic plants. Patent US6091002 assigned to Monsanto Company, St Louis, MO; 2000.
[44] Asrar J, Mitsky TA, Shah DT. Polyhydroxyalkanoates of narrow molecular weight distribution prepared in transgenic plants. Patent US6228623 assigned to Monsanto Company, St Louis, MO; 2001.
[45] El-Hadi A, Schnabel R, Straube E, Müller G, Henning S. Correlation between degree of crystallinity, morphology, glass temperature, mechanical properties and biodegradation of poly(3-hydroxyalkanoate) PHAs and their blends. Polym Test 2002;21:665–74.
[46] Velho L, Velho P. Innovation in resource-based technology clusters: investigating the lateral migration thesis—the development of a sugar-based plastic in Brazil. Report of the Centre for Poverty, Employment and Growth. Published by the Human Science Research Council, Pretoria (South Africa). http://www.hsrc.ac.za/research/output/outputDocuments/4221_Velho_DevelopmentofsugarbasedplasticinBrazil.pdf; 2006.
[47] Noda I, Green PR, Satkowski MM, Schechtman LA. Preparation and properties of a novel class of polyhydroxyalkanoate copolymers. Biomacromolecules 2005;6:580–6.
[48] Philip S, Keshavarz T, Roy I. Polyhydroxyalkanoates: biodegradable polymers with a range of applications. J Chem Technol Biotechnol 2007;82:233–47.
[49] Williams SF, Martin DP, Horowitz DM, Peoples OP. PHA applications: addressing the price performance issue. I. Tissue engineering. Int J Biol Macromol 1999;25:111–21.
[50] Amass W, Amass A, Tighe B. A review of biodegradable polymers: uses, current developments in the synthesis and characterization of biodegradable polyesters, blends of biodegradable polymers and recent advances in biodegradation studies. Polym Int 1998;47:89–144.
[51] Shogren R. Water vapor permeability of biodegradable polymers. J Environ Polym Degrad 1997;5:91–5.
[52] Kotnis MA, O'Brien GS, Willett JL. Processing and mechanical properties of biodegradable poly(hydroxybutyrate-co-valerate)-starch compositions. J Environ Polym Degrad 1995;3:97–105.
[53] Shogren RL. Poly(ethylene oxide)-coated granular starch-poly(hydroxybutyrate-co-hydroxyvalerate) composite materials. J Environ Polym Degrad 1995;3:75–80.
[54] Ramkumar DHS, Bhattacharya M. Steady shear and dynamic properties of biodegradable polyesters. Polym Eng Sci 1998;38:1426–35.
[55] Karlsson S, Albertsson A-C. Biodegradable polymers and environmental interaction. Polym Eng Sci 1998;38:1251–3.
[56] Parikh M, Gross RA, McCarthy SP. The influence of injection molding conditions on biodegradable polymers. J Inject Molding Technol 1998;2:30.
[57] Rosa DS, Calil MR, Guedes CGF, Rodrigues TC. Biodegradability of thermally aged PHB, PHB-V, and PCL in soil compostage. J Polym Environ 2004;12:239–45.
[58] Chiellini E, Solaro R. Biodegradable polymeric materials. Adv Mater 1996;8:305–13.
[59] Bastioli C, Cerutti A, Guanella I, Romano GC, Tosin M. Physical state and biodegradation behavior of starch–polycaprolactone systems. J Environ Polym Degrad 1995;3:81–95.
[60] Bastioli C. Properties and applications of Mater-Bi starch-based materials. Polym Degrad Stabil 1998;59:263–72.
[61] Averous L, Moro L, Dole P, Fringant C. Properties of thermoplastic blends: starch–polycaprolactone. Polymer 2000;41:4157–67.
[62] Koenig MF, Huang SJ. Evaluation of crosslinked poly(caprolactone) as a biodegradable, hydrophobic coating. Polym Degrad Stabil 1994;45:139–44.
[63] Tokiwa Y, Suzuki T. Hydrolysis of polyesters by lipases. Nature 1977;270:76–8.
[64] Lee S-R, Park H-M, Lim H, Kang T, Li X, Cho W-J, et al. Microstructure, tensile properties, and biodegradability of aliphatic polyester/clay nanocomposites. Polymer 2002;43:2495–500.
[65] Muller R-J, Witt U, Rantze E, Deckwer W-D. Architecture of biodegradable copolyesters containing aromatic constituents. Polym Degrad Stabil 1998;59:203–8.
[66] Yokota Y, Marechal H. Processability of biodegradable poly(butylene) succinate and its derivates. A case study. In: Biopolymer Conference, Würzburg (Germany). 1999.
[67] Fujimaki T. Processability and properties of aliphatic polyesters, 'Bionolle', synthesized by polycondensation reaction. Polym Degrad Stabil 1998;59:209–14.
[68] Ratto JA, Stenhouse PJ, Auerbach M, Mitchell J, Farrell R. Processing, performance and biodegradability of a thermoplastic aliphatic polyester/starch system. Polymer 1999;40:6777–88.
[69] Kim J, Shin TK, Choi HJ, Jhon MS. Miscibility of biodegradable synthetic aliphatic polyester and poly(epichlorohydrin) blends. Polymer 1999;40:6873–6.
[70] Kim J, Kim JH, Shin TK, Choi HJ, Jhon MS. Miscibility and rheological characteristics of biodegradable aliphatic polyester and linear low density polyethylene blends. Eur Polym J 2001;37:2131–9.
[71] Kim J, Lim ST, Choi HJ, Jhon MS. Rheological and mechanical characterization of biodegradable aliphatic polyester and poly(epichlorohydrin) blends. Macromol Chem Phys 2001;202:2634–40.
[72] Witt U, Einig T, Yamamoto M, Kleeberg I, Deckwer W-D, Muller R-J. Biodegradation of aliphatic–aromatic copolyesters: evaluation of the final biodegradability and ecotoxicological impact of degradation intermediates. Chemosphere 2001;44:289–99.
[73] Grigat E, Koch R, Timmermann R. BAK 1095 and BAK 2195: completely biodegradable synthetic thermoplastics. Polym Degrad Stabil 1998;59:223–6.
[74] Fritz J. Ecotoxicity of biogenic materials during and after their biodegradation. PhD Thesis. Vienna, Austria: University of Agriculture; 1999.
[75] Bruns C, Gottschall R, De Wilde B. Ecotoxicological trials with BAK 1095 according to DIN V 54900. Orbit J 2001;1:1–10.
[76] Ogata N, Jimenez G, Kawai H, Ogihara T. Structure and thermal/mechanical properties of poly(L-lactide)-clay blend. J Polym Sci Polym Phys 1997;35:389–96.
[77] Chang J-H, An YU, Cho D, Giannelis EP. Poly(lactic acid) nanocomposites: comparison of their properties with montmorillonite and synthetic mica (II). Polymer 2003;44:3715–20.
[78] Chang J-H, An YU, Sur GS. Poly(lactic acid) nanocomposites with various organoclays. I. Thermomechanical properties, morphology, and gas permeability. J Polym Sci Polym Phys 2003;41:94–103.
[79] Krikorian V, Pochan DJ. Poly(L-lactic acid)/layered silicate nanocomposite: fabrication, characterization and properties. Chem Mater 2003;15:4317–24.

[80] Krikorian V, Pochan DJ. Unusual crystallization behavior of organoclay reinforced poly(L-lactic acid) nanocomposites. Macromolecules 2004;37:6480–91.
[81] Krikorian V, Pochan DJ. Crystallization behavior of poly(L-lactic acid) nanocomposites: nucleation and growth probed by infrared spectroscopy. Macromolecules 2005;38:6520–7.
[82] Wu T-M, Wu C-Y. Biodegradable poly(lactic acid)/chitosan-modified montmorillonite nanocomposites: preparation and characterization. Polym Degrad Stabil 2006;91:2198–204.
[83] Pluta M, Galeski A, Alexandre M, Paul M-A, Dubois P. Polylactide/montmorillonite nanocomposites and microcomposites prepared by melt blending: structure and some physical properties. J Appl Polym Sci 2002;86:1497–506.
[84] Maiti P, Giannelis EP, Batt CA. Biodegradable polyester/layered silicate nanocomposites. Mater Res Soc Symp Proc 2002;740:141–5.
[85] Maiti P, Yamada K, Okamoto M, Ueda K, Okamoto K. New polylactide/layered silicate nanocomposites: role of organoclays. Chem Mater 2002;14:4654–61.
[86] Sinha Ray S, Yamada K, Okamoto M, Ueda K. Polylactide-layered silicate nanocomposite: a novel biodegradable material. Nano Lett 2002;2:1093–6.
[87] Sinha Ray S, Yamada K, Ogami A, Okamoto M, Ueda K. New polylactide/layered silicate nanocomposite: nanoscale control over multiple properties. Macromol Rapid Commun 2002;23:943–7.
[88] Sinha Ray S, Maiti P, Okamoto M, Yamada K, Ueda K. New polylactide/layered silicate nanocomposites. 1. Preparation, characterization and properties. Macromolecules 2002;35:3104–10.
[89] Sinha Ray S, Yamada K, Okamoto M, Ueda K. New polylactide-layered silicate nanocomposites. 2. Concurrent improvements of material properties, biodegradability and melt rheology. Polymer 2003;44:857–66.
[90] Sinha Ray S, Yamada K, Okamoto M, Ogami A, Ueda K. New polylactide/layered silicate nanocomposites. 3. High-performance biodegradable materials. Chem Mater 2003;15:1456–65.
[91] Sinha Ray S, Yamada K, Okamoto M, Ogami A, Ueda K. New polylactide/layered silicate nanocomposites. 4. Structure, properties and biodegradability. Compos Interfaces 2003;10:435–50.
[92] Sinha Ray S, Yamada K, Okamoto M, Fujimoto Y, Ogami A, Ueda K. New polylactide/layered silicate nanocomposites. 5. Designing of materials with desired properties. Polymer 2003;44:6633–46.
[93] Sinha Ray S, Okamoto M. New polylactide/layered silicate nanocomposites. 6. Melt rheology and foam processing. Macromol Mater Eng 2003;288:936–44.
[94] Sinha Ray S, Okamoto M. Biodegradable polylactide and its nanocomposites: opening a new dimension for plastics and composites. Macromol Rapid Commun 2003;24:815–40.
[95] Sinha Ray S, Yamada K, Okamoto M, Ueda K. Biodegradable polylactide/montmorillonite nanocomposites. J Nanosci Nanotechnol 2003;3:503–10.
[96] Nam PH, Fujimori A, Masuko T. Flocculation characteristics of organo-modified clay particles in poly(L-lactide)/montmorillonite hybrid systems. e-Polymers 2004, no. 005.
[97] Nam PH, Fujimori A, Masuko T. The dispersion behavior of clay particles in poly(L-lactide)/organo-modified montmorillonite hybrid systems. J Appl Polym Sci 2004;93:2711–20.
[98] Paul M-A, Delcourt C, Alexandre M, Degée P, Monteverde F, Dubois P. Polylactide/montmorillonite nanocomposites: study of the hydrolytic degradation. Polym Degrad Stabil 2005;87:535–42.
[99] Yoshida O, Okamoto M. Direct melt intercalation of polylactide chains into nano-galleries: interlayer expansion and nanocomposite structure. Macromol Rapid Commun 2006;27:751–7.
[100] Nam JY, Sinha Ray S, Okamoto M. Crystallization behavior and morphology of biodegradable polylactide/layered silicate nanocomposite. Macromolecules 2003;36:7126–31.
[101] Sinha Ray S, Yamada K, Okamoto M, Ueda K. Control of biodegradability of polylactide via nanocomposite technology. Macromol Mater Eng 2003;288:203–8.
[102] Chen G-X, Kim H-S, Kim E-S, Yoon J-S. Compatibilization-like effect of reactive organoclay on the poly(L-lactide)/poly(butylene succinate) blends. Polymer 2005;46:11829–36.
[103] Chen G-X, Yoon J-S. Thermal stability of poly(L-lactide)/poly (butylene succinate)/clay nanocomposites. Polym Degrad Stabil 2005;88:206–12.
[104] Lewitus D, McCarthy S, Ophir A, Kenig S. The effect of nanoclays on the properties of PLLA-modified polymers Part 1: mechanical and thermal properties. J Polym Environ 2006;14:171–7.
[105] Hasook A, Tanoue S, Lemoto Y, Unryu T. Characterization and mechanical properties of poly(lactic acid)/poly(ε-caprolactone)/organoclay nanocomposites prepared by melt compounding. Polym Eng Sci 2006;46:1001–7.
[106] Paul M-A, Alexandre M, Degée P, Henrist C, Rulmont A, Dubois P. New nanocomposite materials based on plasticized poly(L-lactide) and organo-modified montmorillonites: thermal and morphological study. Polymer 2003;44:443–50.
[107] Pluta M. Morphology and properties of polylactide modified by thermal treatment, filling with layered silicates and plasticization. Polymer 2004;45:8239–51.
[108] Paul M-A, Delcourt C, Alexandre M, Degée P, Monteverde F, Rulmont A, et al. (Plasticized) polylactide/(organo-)clay nanocomposites by in situ intercalative polymerization. Macromol Chem Phys 2005;206:484–98.
[109] Pluta M, Paul M-A, Alexandre M, Dubois P. Plasticized polylactide/clay nanocomposites. I. The role of filler content and its surface organo-modification on the physico-chemical properties. J Polym Sci Polym Phys 2006;44:299–311.
[110] Pluta M, Paul M-A, Alexandre M, Dubois P. Plasticized polylactide/clay nanocomposites. II. The effect of aging on structure and properties in relation to the filler content and the nature of its organo-modification. J Polym Sci Polym Phys 2006;44:312–25.
[111] Tanoue S, Hasook A, Iemoto Y, Unryu T. Preparation of poly(lactic acid)/poly(ethylene glycol)/organoclay nanocomposites by melt compounding. Polym Compos 2006;27:256–63.
[112] Shibata M, Someya Y, Orihara M, Miyoshi M. Thermal and mechanical properties of plasticized poly(L-lactide) nanocomposites with organo-modified montmorillonites. J Appl Polym Sci 2006;99:2594–602.
[113] Paul M-A, Alexandre M, Degée P, Calberg C, Jerome R, Dubois P. Exfoliated polylactide/clay nanocomposites by in-situ coordination-insertion polymerization. Macromol Rapid Commun 2003;24:561–6.
[114] Sinha Ray S, Okamoto K, Yamada K, Okamoto M. Novel porous ceramic material via burning of polylactide/layered silicate nanocomposite. Nano Lett 2002;2:423–5.
[115] Lee JH, Park TG, Park HS, Lee DS, Lee YK, Yoon SC, et al. Thermal and mechanical characteristics of poly(L-lactic acid) nanocomposite scaffold. Biomaterials 2003;24:2773–8.
[116] Lee YH, Lee JH, An I-G, Kim C, Lee DS, Lee YK, et al. Electrospun dual-porosity structure and biodegradation morphology of Montmorillonite reinforced PLLA nanocomposite scaffolds. Biomaterials 2005;26:3165–72.
[117] Ema Y, Ikeya M, Okamoto M. Foam processing and cellular structure of polylactide-based nanocomposites. Polymer 2006;47:5350–9.
[118] Maiti P, Batt CA, Giannelis EP. Renewable plastics: synthesis and properties of PHB nanocomposites. Polym Mater Sci Eng 2003;88:58–9.
[119] Hablot E, Bordes P, Pollet E, Avérous L. Thermal and thermo-mechanical degradation of PHB-based multiphase systems. Polym Degrad Stabil 2008;93:413–21.
[120] Lim ST, Hyun YH, Lee CH, Choi HJ. Preparation and characterization of microbial biodegradable poly(3-hydroxybutyrate)/organoclay nanocomposite. J Mater Sci Lett 2003;22:299–302.
[121] Choi WM, Kim TW, Park OO, Chang YK, Lee JW. Preparation and characterization of poly(hydroxybutyrate-co-hydroxyvalerate)-organoclay nanocomposites. J Appl Polym Sci 2003;90:525–9.
[122] Wang S, Song C, Chen G, Guo T, Liu J, Zhang B, et al. Characteristics and biodegradation properties of poly(3-hydroxybutyrate-co-3-hydroxyvalerate)/organophilic montmorillonite (PHBV/OMMT) nanocomposite. Polym Degrad Stabil 2005;87:69–76.
[123] Chen GX, Hao GJ, Guo TY, Song MD, Zhang BH. Crystallization kinetics of poly(3-hydroxybutyrate-co-3-hydroxyvalerate)/clay nanocomposites. J Appl Polym Sci 2004;93:655–61.
[124] Chen GX, Hao GJ, Guo TY, Song MD, Zhang BH. Structure and mechanical properties of poly(3-hydroxybutyrate-co-3-hydroxyvalerate) (PHBV)/clay nanocomposites. J Mater Sci Lett 2002;21:1587–9.
[125] Misra M, Desai SM, Mohanty AK, Drzal LT. Novel solvent-free method for functionalization of polyhydroxyalkanoates: synthesis and characterizations. In: Proceedings of the 62nd annual technical conference of the society of plastics engineers, vol.2. Boca Raton (FL), USA: CRC Press; 2004. p. 2442–6.
[126] Drzal LT, Misra M, Mohanty AK. Sustainable biodegradable green nanocomposites from bacterial bioplastic for automotive applications. In: Proceedings of the US EPA 2004 STAR progress review workshop – nanotechnology and the environment II. Washington, DC (USA): Published by US Environmental Protection Agency. Report number EPA/600/R-05/089;

2005. p 23–5. http://es.epa.gov/ncer/nano/publications/8-18-04/fnanoproc_092005.pdf.
[127] Messersmith PB, Giannelis EP. Synthesis and barrier properties of polycaprolactone-layered silicate nanocomposites. J Polym Sci Polym Chem 1995;33:1047–57.
[128] Messersmith PB, Giannelis EP. Polymer-layered silicate nanocomposites: in situ intercalative polymerization of ε-caprolactone in layered silicates. Chem Mater 1993;5:1064–6.
[129] Krishnamoorti R, Giannelis EP. Rheology of end-tethered polymer layered silicate nanocomposites. Macromolecules 1997;30:4097–102.
[130] Kiersnowski A, Dabrowski P, Budde H, Kressler J, Piglowski J. Synthesis and structure of poly(ε-caprolactone)/synthetic montmorillonite nano-intercalates. Eur Polym J 2004;40:2591–8.
[131] Kiersnowski A, Piglowski J. Polymer-layered silicate nanocomposites based on poly(ε-caprolactone). Eur Polym J 2004;40:1199–207.
[132] Pucciariello R, Villani V, Belviso S, Gorrasi G, Tortora M, Vittoria V. Phase behavior of modified montmorillonite-poly(ε-caprolactone) nanocomposites. J Polym Sci Polym Phys 2004;42:1321–32.
[133] Pucciariello R, Villani V, Langerame F, Gorrasi G, Vittoria V. Interfacial effects in organophilic montmorillonite-poly(ε-caprolactone) nanocomposites. J Polym Sci Polym Phys 2004;42:3907–19.
[134] Tortora M, Vittoria V, Galli G, Ritrovati S, Chiellini E. Transport properties of modified montmorillonite-poly(ε-caprolactone) nanocomposites. Macromol Mater Eng 2002;287:243–9.
[135] Pantoustier N, Lepoittevin B, Alexandre M, Kubies D, Calberg C, Jerome R, et al. Biodegradable polyester layered silicate nanocomposites based on poly(ε-caprolactone). Polym Eng Sci 2002;42:1928–37.
[136] Kubies D, Pantoustier N, Dubois P, Rulmont A, Jerome R. Controlled ring-opening polymerization of ε-caprolactone in the presence of layered silicates and formation of nanocomposites. Macromolecules 2002;35:3318–20.
[137] Lepoittevin B, Pantoustier N, Devalckenaere M, Alexandre M, Kubies D, Calberg C, et al. Poly(ε-caprolactone)/clay nanocomposites by in-situ intercalative polymerization catalyzed by dibutyltin dimethoxide. Macromolecules 2002;35:8385–90.
[138] Lepoittevin B, Pantoustier N, Alexandre M, Calberg C, Jerome R, Dubois P. Polyester layered silicate nanohybrids by controlled grafting polymerization. J Mater Chem 2002;12:3528–32.
[139] Lepoittevin B, Pantoustier N, Alexandre M, Calberg C, Jerome R, Dubois P. Layered silicate/polyester nanohybrids by controlled ring-opening polymerization. Macromol Symp 2002;183:95–102.
[140] Pantoustier N, Alexandre M, Degée P, Kubies D, Jerome R, Henrist C, et al. Intercalative polymerization of cyclic esters in layered silicates: thermal vs catalytic activation. Compos Interfaces 2003;10:423–33.
[141] Viville P, Lazzaroni R, Pollet E, Alexandre M, Dubois P, Borcia G, et al. Surface characterization of poly(ε-caprolactone)-based nanocomposites. Langmuir 2003;19:9425–33.
[142] Gorrasi G, Tortora M, Vittoria V, Pollet E, Lepoittevin B, Alexandre M, et al. Vapor barrier properties of polycaprolactone montmorillonite nanocomposites: effect of clay dispersion. Polymer 2003;44:2271–9.
[143] Viville P, Lazzaroni R, Pollet E, Alexandre M, Dubois P. Controlled polymer grafting on single clay nanoplatelets. J Am Chem Soc 2004;126:9007–12.
[144] Pantoustier N, Alexandre M, Degée P, Calberg C, Jerome R, Henrist C, et al. Poly(ε-caprolactone) layered silicate nanocomposites: effect of clay surface modifiers on the melt intercalation process. e-Polymers 2001, no. 009.
[145] Lepoittevin B, Devalckenaere M, Pantoustier N, Alexandre M, Kubies D, Calberg C, et al. Poly(ε-caprolactone)/clay nanocomposites prepared by melt intercalation: mechanical, thermal and rheological properties. Polymer 2002;43:4017–23.
[146] Chen B, Evans JRG. Poly(ε-caprolactone)-clay nanocomposites: structure and mechanical properties. Macromolecules 2006;39:747–54.
[147] Kwak S-Y, Oh KS. Effect of thermal history on structural changes in melt-intercalated poly(ε-caprolactone)/organoclay nanocomposites investigated by dynamic viscoelastic relaxation measurements. Macromol Mater Eng 2003;288:503–8.
[148] Di Y, Iannace S, Di MaioE, Nicolais L. Nanocomposites by melt intercalation based on polycaprolactone and organoclay. J Polym Sci Polym Phys 2003;41:670–8.
[149] Di Maio E, Iannace S, Sorrentino L, Nicolais L. Isothermal crystallization in PCL/clay nanocomposites investigated with thermal and rheometric methods. Polymer 2004;45:8893–900.
[150] Lepoittevin B, Pantoustier N, Devalckenaere M, Alexandre M, Calberg C, Jerome R, et al. Polymer/layered silicate nanocomposites by combined intercalative polymerization and melt intercalation: a masterbatch process. Polymer 2003;44:2033–40.
[151] Shibata M, Teramoto N, Someya Y, Tsukao R. Nanocomposites based on poly(ε-caprolactone) and the montmorillonite treated with dibutylamine-terminated e-caprolactone oligomer. J Appl Polym Sci 2007;104:3112–9.
[152] Kim SW, Jo WH, Lee MS, Ko MB, Jho JY. Preparation of clay-dispersed poly(styrene-co-acrylonitrile) nanocomposites using poly(ε-caprolactone) as a compatibilizer. Polymer 2001;42:9837–42.
[153] Gonzalez I, Eguiazabal JI, Nazabal J. New clay-reinforced nanocomposites based on a polycarbonate/polycaprolactone blend. Polym Eng Sci 2006;46:864–73.
[154] Zheng X, Wilkie CA. Nanocomposites based on poly(ε-caprolactone) (PCL)/clay hybrid: polystyrene, high impact polystyrene, ABS, polypropylene and polyethylene. Polym Degrad Stabil 2003;82:441–50.
[155] Pollet E, Delcourt C, Alexandre M, Dubois P. Transesterification catalysts to improve clay exfoliation in synthetic biodegradable polyester nanocomposites. Eur Polym J 2006;42:1330–41.
[156] Kalambur SB, Rizvi SS. Starch-based nanocomposites by reactive extrusion processing. Polym Int 2004;53:1413–6.
[157] Yoshioka M, Takabe K, Sugiyama J, Nishio Y. Newly developed nanocomposites from cellulose acetate/layered silicate/poly(ε-caprolactone): synthesis and morphological characterization. J Wood Sci 2006;52:121–7.
[158] Maiti P. Influence of miscibility on viscoelasticity, structure, and intercalation of oligo-poly(caprolactone)/layered silicate nanocomposites. Langmuir 2003;19:5502–10.
[159] Calberg C, Jerome R, Grandjean J. Solid-state NMR study of poly(ε-caprolactone)/clay nanocomposites. Langmuir 2004;20:2039–41.
[160] Gardebien F, Gaudel-Siri A, Bredas J-L, Lazzaroni R. Molecular dynamics simulations of intercalated poly(ε-caprolactone)-montmorillonite clay nanocomposites. J Phys Chem B 2004;108:10678–86.
[161] Gardebien F, Bredas J-L, Lazzaroni R. Molecular dynamics simulations of nanocomposites based on poly(ε-caprolactone) grafted on montmorillonite clay. J Phys Chem B 2005;109:12287–96.
[162] Hrobarikova J, Robert J-L, Calberg C, Jerome R, Grandjean J. Solid-state NMR study of intercalated species in poly(ε-caprolactone)/clay nanocomposites. Langmuir 2004;20:9828–33.
[163] Urbanczyk L, Hrobarikova J, Calberg C, Jerome R, Grandjean J. Motional heterogeneity of intercalated species in modified clays and poly(ε-caprolactone)/clay nanocomposites. Langmuir 2006;22:4818–24.
[164] Jimenez G, Ogata N, Kawai H, Ogihara T. Structure and thermal/mechanical properties of poly(ε-caprolactone)-clay blend. J Appl Polym Sci 1997;64:2211–20.
[165] Sinha Ray S, Okamoto K, Maiti P, Okamoto M. New poly(butylene succinate)/layered silicate nanocomposites: Preparation and mechanical properties. J Nanosci Nanotechnol 2002;2:171–6.
[166] Okamoto K, Ray SS, Okamoto M. New poly(butylene succinate)/layered silicate nanocomposites. II. Effect of organically modified layered silicates on structure, properties, melt rheology, and biodegradability. J Polym Sci Polym Phys 2003;41:3160–72.
[167] Sinha Ray S, Okamoto K, Okamoto M. Structure-property relationship in biodegradable poly(butylene succinate)/layered silicate nanocomposites. Macromolecules 2003;36:2355–67.
[168] Sinha Ray S, Okamoto K, Okamoto M. Structure and properties of nanocomposites based on poly(butylene succinate) and organically modified montmorillonite. J Appl Polym Sci 2006;102:777–85.
[169] Someya Y, Nakazato T, Teramoto N, Shibata M. Thermal and mechanical properties of poly(butylene succinate) nanocomposites with various organo-modified montmorillonites. J Appl Polym Sci 2004;91:1463–75.
[170] Chen G-X, Kim E-S, Yoon J-S. Poly(butylene succinate)/twice functionalized organoclay nanocomposites: Preparation, characterization, and properties. J Appl Polym Sci 2005;98:1727–32.
[171] Chen G-X, Yoon J-S. Non-isothermal crystallization kinetics of poly(butylene succinate) composites with a twice functionalized organoclay. J Polym Sci Polym Phys 2005;43:817–26.
[172] Shih YF, Wang TY, Jeng RJ, Wu JY, Teng CC. Biodegradable nanocomposites based on poly(butylene succinate)/organoclay. J Polym Environ 2007;15:151–8.
[173] Sinha Ray S, Bousmina M, Okamoto K. Structure and properties of nanocomposites based on poly(butylene succinate-co-adipate)

and organically modified montmorillonite. Macromol Mater Eng 2005;290:759–68.
[174] Sinha Ray S, Bousmina M. Poly(butylene sucinate-co-adipate)/montmorillonite nanocomposites: effect of organic modifier miscibility on structure, properties, and viscoelasticity. Polymer 2005;46:12430–9.
[175] Sinha Ray S, Bandyopadhyay J, Bousmina M. Effect of organoclay on the morphology and properties of poly(propylene)/poly[(butylene succinate)-co-adipate] blends. Macromol Mater Eng 2007;292: 729–47.
[176] Sinha Ray S, Bandyopadhyay J, Bousmina M. Thermal and thermomechanical properties of poly[(butylene succinate)-co-adipate] nanocomposite. Polym Degrad Stabil 2007;92:802–12.
[177] Lee CH, Lim ST, Hyun YH, Choi HJ, Jhon MS. Fabrication and viscoelastic properties of biodegradable polymer/organophilic clay nanocomposites. J Mater Sci Lett 2003;22:53–5.
[178] Lim ST, Hyun YH, Choi HJ, Jhon MS. Synthetic biodegradable aliphatic polyester/montmorillonite nanocomposites. Chem Mater 2002;14:1839–44.
[179] Lim ST, Lee CH, Choi HJ, Jhon MS. Solid-like transition of melt-intercalated biodegradable polymer/clay nanocomposites. J Polym Sci Polym Phys 2003;41:2052–61.
[180] Lim ST, Lee CH, Kim HB, Choi HJ, Jhon MS. Polymer/organoclay nanocomposites with biodegradable aliphatic polyester and its blends: preparation and characterization. e-Polymers 2004, no. 026.
[181] Lee CH, Kim HB, Lim ST, Choi HJ, Jhon MS. Biodegradable aliphatic polyester-poly(epichlorohydrin) blend/organoclay nanocomposites: synthesis and rheological characterization. J Mater Sci 2005;40:3981–5.
[182] Chen G, Yoon J-S. Nanocomposites of poly[(butylene succinate)-co-(butylene adipate)](PBSA) and twice-functionalized organoclay. Polym Int 2005;54:939–45.
[183] Sinha Ray S, Bousmina M. Crystallization behavior of poly[(butylene succinate)-co-adipate] nanocomposite. Macromol Chem Phys 2006;207:1207–19.
[184] Someya Y, Sugahara Y, Shibata M. Nanocomposites based on poly(butylene adipate-co-terephthalate) and montmorillonite. J Appl Polym Sci 2005;95:386–92.
[185] Someya Y, Kondo N, Teramoto N, Shibata M. Studies of biodegradation of poly (butylene adipate-co-butylene terephtharate)/layered silicate nanocomposites. Polym Prepr Jpn 2005;54:5362.
[186] Chivrac F, Kadlecova Z, Pollet E, Averous L. Aromatic copolyester-based nano-biocomposites: elaboration, structural characterization and properties. J Polym Environ 2006;14:393–401.
[187] Chivrac F, Pollet E, Averous L. Nonisothermal crystallization behavior of poly(butylene adipate-co-terephthalate)/clay nano-biocomposites. J Polym Sci Polym Phys 2007;45:1503–10.
[188] Krook M, Albertsson A-C, Gedde UW, Hedenqvist MS. Barrier and mechanical properties of montmorillonite/polyesteramide nanocomposites. Polym Eng Sci 2002;42:1238–46.
[189] Krook M, Morgan G, Hedenqvist MS. Barrier and mechanical properties of injection molded montmorillonite/polyesteramide nanocomposites. Polym Eng Sci 2005;45:135–41.
[190] Averous L. Biodegradable multiphase systems based on plasticized starch: a review. J Macromol Sci Polym Rev 2004;C44:231–74.
[191] Lagaly G. From clay mineral crystals to colloidal clay mineral dispersions. In: Dobias B, editor. Coagulation and flocculation—theory and applications. New York: Dekker; 1993. p. 427.
[192] Sinha Ray S, Okamoto M. Polymer/layered silicate nanocomposites: a review from preparation to processing. Prog Polym Sci 2003;28:1539–641.
[193] Utracki LA, Sepehr M, Boccaleri E. Synthetic, layered nanoparticles for polymeric nanocomposites (PNCs). Polym Adv Technol 2007;18:1–37.